NRL Report 7795

Calculations of Multipath Range Errors For Variations in Design of the Extended Area Tracking System (EATS)

DAVID C. CROSS

Search Radar Branch
Radar Division

September 27, 1974

NAVAL RESEARCH LABORATORY
Washington, D.C.

SECURITY CLASSIFICATION OF THIS PAGE *(When Data Entered)*

REPORT DOCUMENTATION PAGE		READ INSTRUCTIONS BEFORE COMPLETING FORM
1. REPORT NUMBER NRL Report 7795	2. GOVT ACCESSION NO.	3. RECIPIENT'S CATALOG NUMBER
4. TITLE *(and Subtitle)* CALCULATIONS OF MULTIPATH RANGE ERRORS FOR VARIATIONS IN DESIGN OF THE EXTENDED AREA TRACKING SYSTEM (EATS)		5. TYPE OF REPORT & PERIOD COVERED Interim report on the NRL problem. 6. PERFORMING ORG. REPORT NUMBER
7. AUTHOR(s) David C. Cross		8. CONTRACT OR GRANT NUMBER(s)
9. PERFORMING ORGANIZATION NAME AND ADDRESS Naval Research Laboratory Washington, D. C. 20375		10. PROGRAM ELEMENT, PROJECT, TASK AREA & WORK UNIT NUMBERS NRL Problem R02-24 A-5355352-652E-4F09905000
11. CONTROLLING OFFICE NAME AND ADDRESS Department of the Navy Naval Air Systems Command Arlington, Virginia 20361		12. REPORT DATE September 27, 1974 13. NUMBER OF PAGES 44
14. MONITORING AGENCY NAME & ADDRESS*(if different from Controlling Office)*		15. SECURITY CLASS. *(of this report)* Unclassified 15a. DECLASSIFICATION/DOWNGRADING SCHEDULE

16. DISTRIBUTION STATEMENT *(of this Report)*

Approved for public release; distribution unlimited.

17. DISTRIBUTION STATEMENT *(of the abstract entered in Block 20, if different from Report)*

18. SUPPLEMENTARY NOTES

19. KEY WORDS *(Continue on reverse side if necessary and identify by block number)*

Range tracking
Range error
Multipath error
FM/CW
Split-gate tracker
Leading-edge tracker
Biphase modulation

20. ABSTRACT *(Continue on reverse side if necessary and identify by block number)*

A basic limitation to the Pacific Missile Range's (PMR's) proposed Extended Area Tracking System (EATS) is multipath range error caused by sea-surface reflections. NRL undertook a study to determine the effect of multipath on the performance of EATS. The study was aimed at generating data as a function of design factors to assist PMR in specifying an optimum EATS system. The system design factors investigated include system RF bandwidth, RF frequency, height of all relay aircraft, polarization, modulation technique, and tracking technique. The data from this study were presented in the form

DD FORM 1 JAN 73 1473 EDITION OF 1 NOV 65 IS OBSOLETE
S/N 0102-014-6601

SECURITY CLASSIFICATION OF THIS PAGE *(When Data Entered)*

20.

of computer-drawn error contour plots which describe the region of the missile range where errors exceed a given magnitude. A subset of these plots was examined for each factor under study to determine the effect of that factor on the range measurement errors. One result of this study indicates that an optimum system under the worst conditions may have an rms range error as large as 250 feet in some regions of the coverage area. The results show that an optimum system should have the widest feasible bandwidth, choose a 25,000-foot relay-aircraft altitude, use vertical polarization, use the leading-edge tracking technique, and have a narrow ground-station-antenna beamwidth.

CONTENTS

CALCULATIONS OF MULTIPATH RANGE ERRORS FOR VARIATIONS IN DESIGN OF THE EXTENDED AREA TRACKING SYSTEM (EATS)

INTRODUCTION

The Pacific Missile Range (PMR) with the assistance of the Stanford Research Institute (SRI) conceived an Extended Area Tracking System (EATS) to accurately locate multiple targets within a missile range about 150 n.mi. wide by 200 n.mi. long [1]. The EATS is a bilateration scheme aided by target altimeter data. The basic bilateration is between two (or more) relay aircraft and a target with a transponder. The transponder is interrogated by and responds with signals for range measurement. The responding signal also contains the altitude measured by a device on the target.

The accuracy of EATS is limited primarily by the errors caused by interference of the signal reflected from the sea surface with the desired direct signal. NRL initially estimated this multipath range error to be about 100 to 200 feet rms for typical system parameters. Because this is a fundamental limitation to accuracy, NRL was requested to analyze the multipath range errors for various possible designs of the EATS system to aid PMR in selecting an optimum system. The design factors investigated were:

System bandwidth,
RF frequency,
Height of the relay aircraft,
Polarization,
Modulation technique,
Tracking technique.

Range errors were calculated for each system as a function of the target's location in the operating range. The error at a given point depends on the relative phase and relative amplitude of the direct and indirect signals. These quantities were determined from the EATS geometry. The calculations used a curved earth model in determining path lengths and scattering from the earth's surface. As the phase varies, the error will vary cyclicly. The rms and peak values of this error function were then calculated and presented in contour plots. (Contour plots of peak errors are not included in this report.) Each contour bounds the portion of the coverage area where the peak or rms error exceeds a certain value. Further details concerning the method of calculating the range error and the method of plotting the contours will be discussed following a description of the range tracking systems that were simulated and studies of the plots themselves to determine the effects of the preceding design factors and other factors.

Note: Manuscript submitted July 16, 1974

SIMULATION OF RANGE TRACKING SYSTEMS

Leading-Edge Tracker

A leading-edge tracker measures the time delay between the time a pulse is transmitted until the leading edge of the target echo is received. Usually the time of arrival of the leading edge is detected by a threshold detector which is enabled by a range gate. During the time the range gate is present, the threshold circuit examines the return signal to determine if it exceeds a preset threshold value. The time at which the threshold value is exceeded is defined as the time of arrival of the leading edge of the return echo. To maximize the sensitivity of the threshold detector, the threshold level is chosen so that the threshold occurs where the rise of the pulse has its steepest slope. This requires that during the operation the pulse amplitude must be normalized by an AGC circuit. Mathematically this is equivalent to finding the time within the range gate when the derivative of the return has its maximum positive slope. This procedure is discussed in Ref [2].

In the EATS study a Gaussian pulse shape was assumed. The received signal was calculated as the linear detected sum of the direct and indirect signal described earlier. The derivatives of this function were examined to find the time at which the maximum slope occurred. This time was then compared to the time obtained if no multipath interference existed. The difference between these two times expressed in feet was taken as the range error.

Centroid Tracker

A centroid tracker measures the time delay between the time a pulse is transmitted until the center of gravity of the target echo is received. The time of arrival of the center of gravity is detected by a split-gate integrating operation. The range gate is divided into two halves called the early and late gates. For the EATS simulation the target return, calculated as was described, was integrated during each gate. The resulting integrals were then compared. If the integrals were not equal, both gates were moved together until equality was achieved. The time associated with the center of the gates, when equality was achieved, was considered the time of arrival of the return. This time was then compared to the time obtained if no multipath interference existed. The difference between these two times expressed in feet was taken as the range error.

Frequency-Modulated Continuous-Wave (FM/CW) Tracker

An FM/CW tracker transmits a frequency-modulated RF carrier. On reception of the echo the phase of the detected modulating function is compared with the phase of the modulation function currently being transmitted. The difference in phase angle is a direct measure of the target's range. If the receiver is assumed to contain a perfect limiter and a linear FM discriminator, an expression for range errors caused by multipath interference can be derived. This has been done by several authors [3-5]. A complete derivation of the range errors is given by Sollenberger [5]. For the EATS study this expression was programmed and used to simulate an FM/CW ranging system.

Biphase-Modulation Tracker

The biphase-modulation technique is used in the Integrated Target Control System (ITCS). It is a combination of an FM/CW tracker and a phase-modulated tracker. A phase-modulated tracker transmits a phase-modulated RF carrier. On reception of the return echo the modulating function is detected using a phase detector. The phase of the detected modulation function is then compared with the phase of the modulation function being transmitted. Just as in the FM/CW system the phase difference is a direct measure of the target's range. The ITCS system uses an FM/CW technique for the uplink from ground control station to the drone being controlled. On the downlink to the ground station, a phase-modulated signal is transmitted. For sinusoidal phase modulation the range errors are of exactly the same form as the FM/CW case. For this reason the ITCS system was treated as a special case of the FM/CW analysis. A derivation of sinusoidal-phase-modulation range error is given in Appendix A. This derivation parallels the work done by Sollenberger [5].

DEPENDENCE OF PERFORMANCE ON DESIGN FACTORS

Plots were generated to demonstrate the effect of changing the factors given in the preceding list. Also, the effect of different sea states on the errors was investigated. Since a complete investigation of all possible combinations of the various factors would have been too expensive, a reduced number of plots were generated. An effort was made to provide a sufficient number of plots to reliably predict the effect each factor has on the multipath range errors. The general approach for testing each design factor was to hold all other factors constant while changing only the factor under investigation. The resulting series of plots can then be compared to observe the effect of that design factor. Typically factors not under control of the EATS designer, such as the polarization of antennas on tracked objects and the sea state, were chosen to produce a worst case and a best case. The worst case was not chosen however if it could obviously be avoided in the final EATS design.

Since many plots were required to complete the study (Figs. 1 through 52), tabulations to index the plots will be provided for the factors investigated, including those not under the control of the designer. The tables (Tables 1 through 6) will be referred to at the beginning of each of the following subsections. The tables indicate the values of the factors and are intended to allow a quick overview of the plots chosen to study each factor.

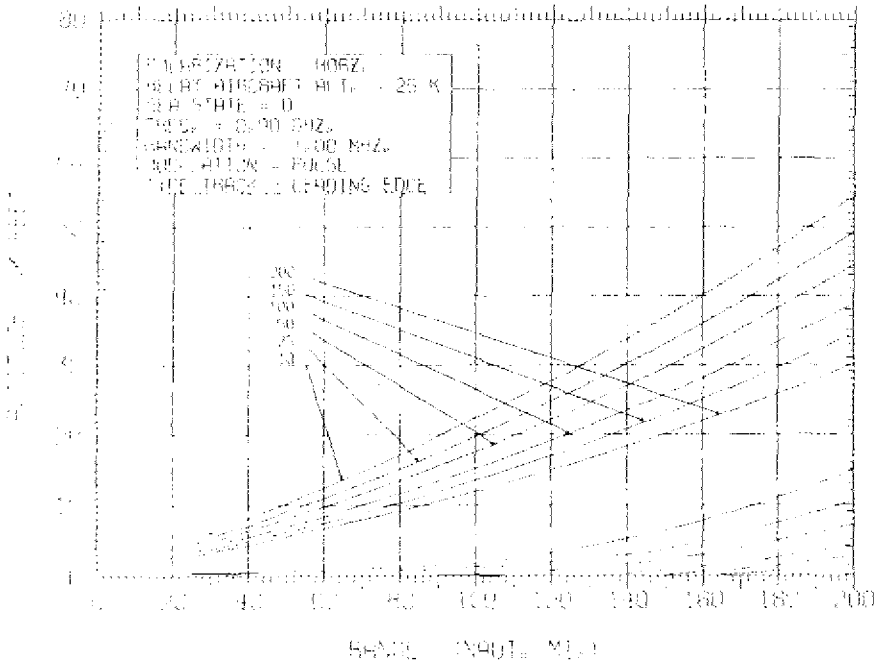

Fig. 1 — Contours of rms range errors (in feet) as a function of target location for the factors listed in the insert. (The lowest labeled curve would connect at the left with the highest unlabeled curve to form the 200-foot contour.)

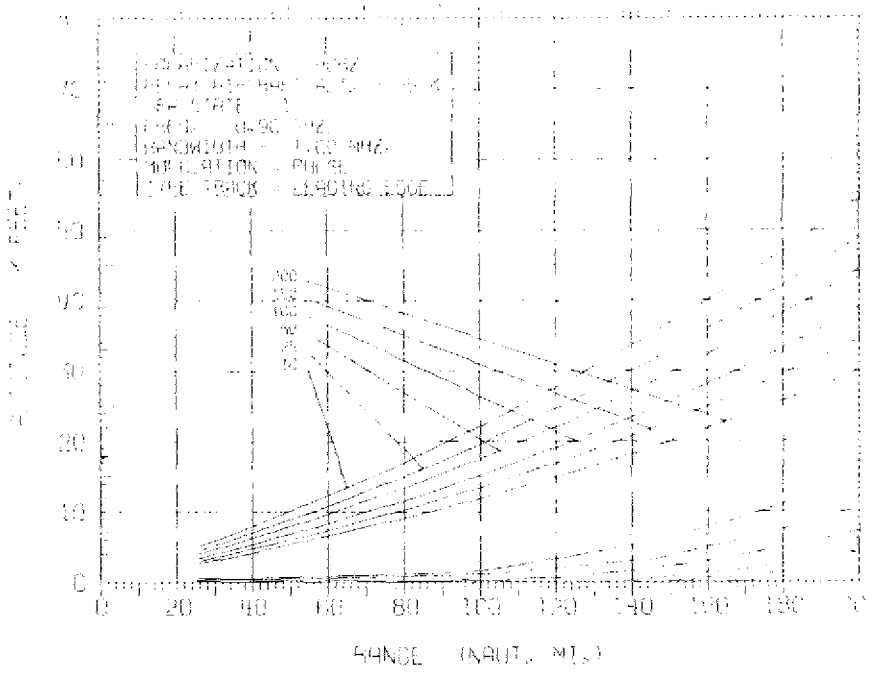

Fig. 2 — Contours of rms range errors

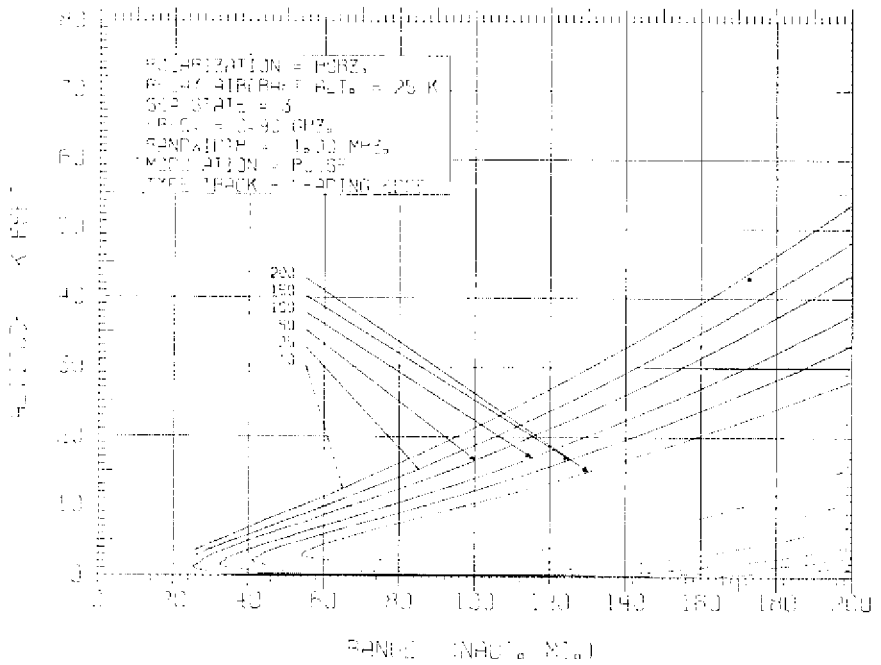

Fig. 3 — Contours of rms range errors

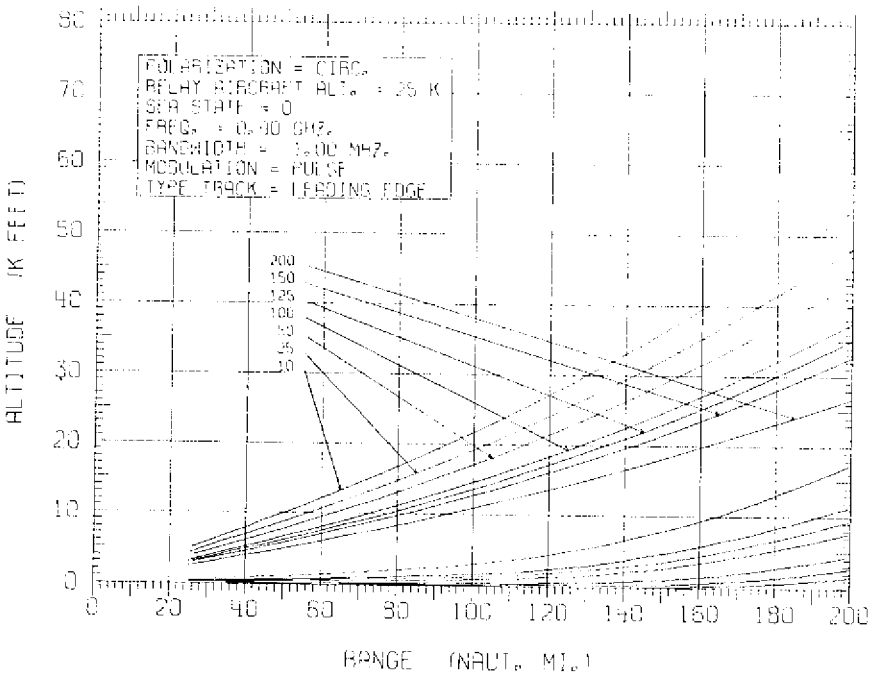

Fig. 4 — Contours of rms range errors

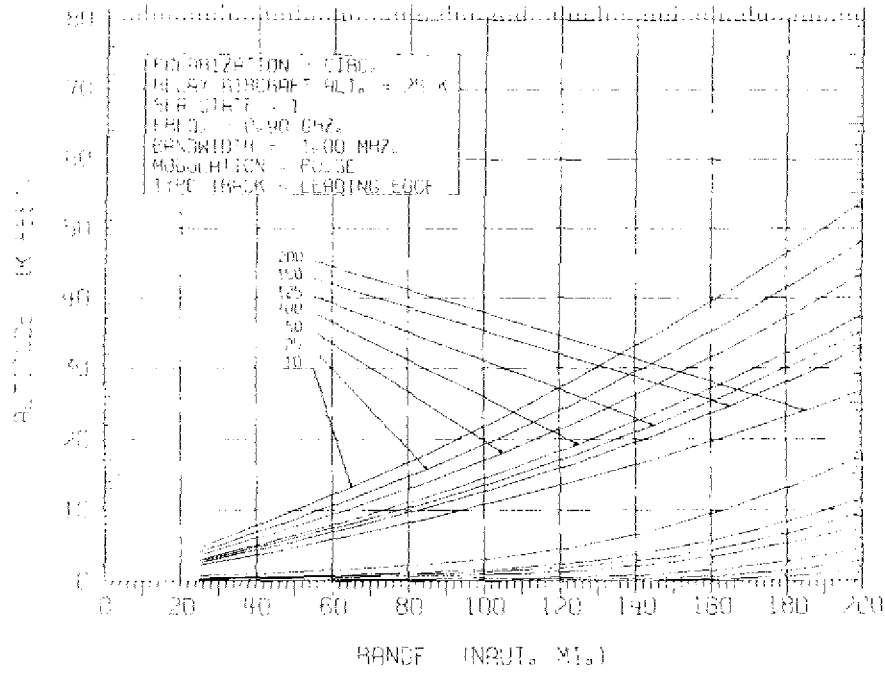

Fig. 5 — Contours of rms range errors

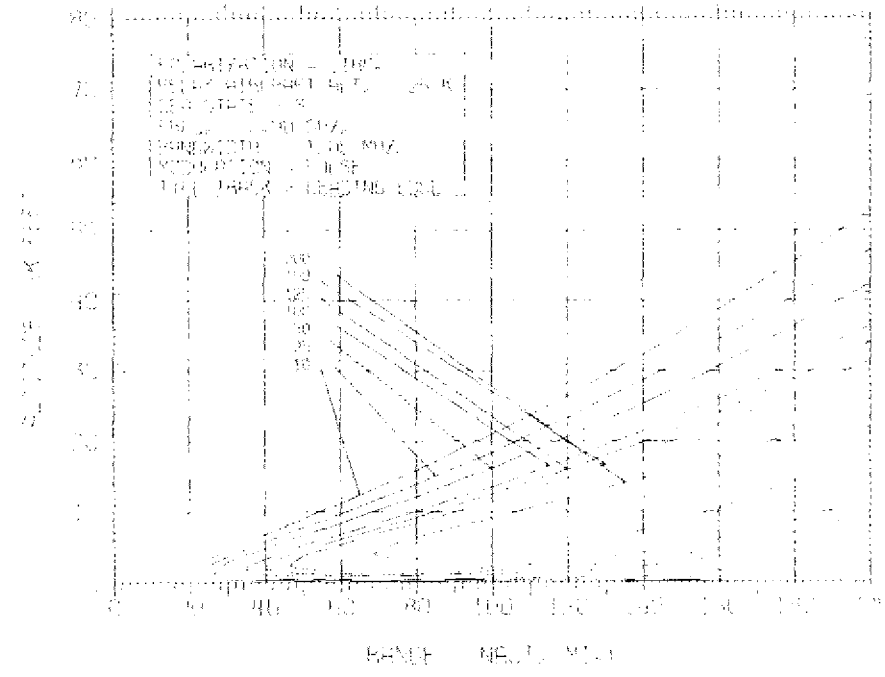

Fig. 6 — Contours of rms range errors

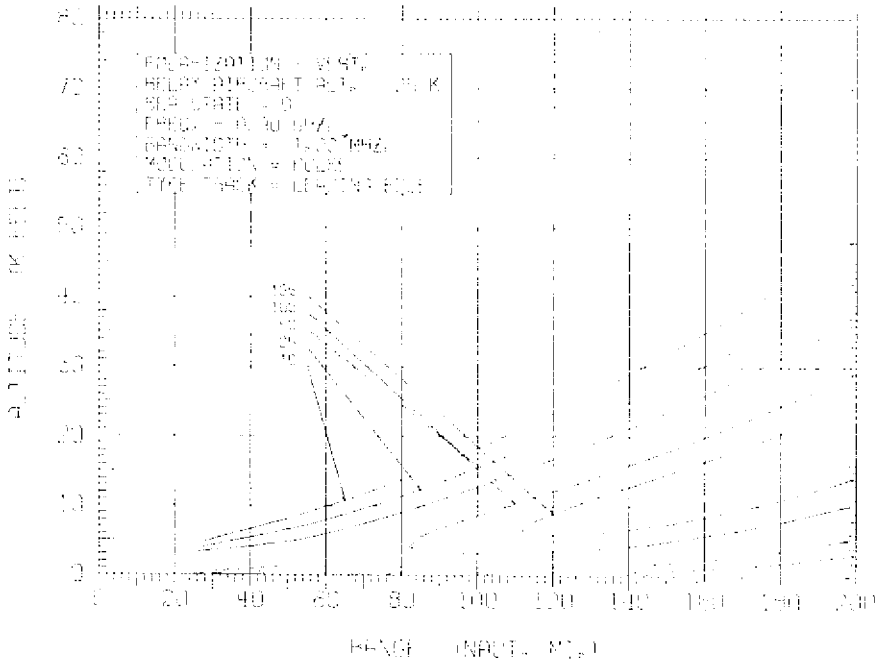

Fig. 7 — Contours of rms range errors

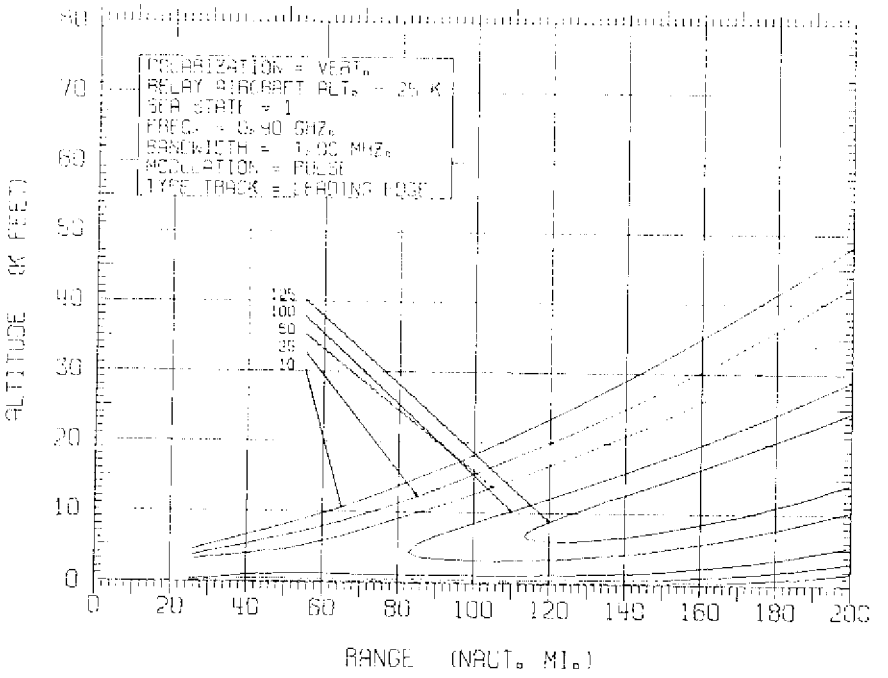

Fig. 8 — Contours of rms range errors

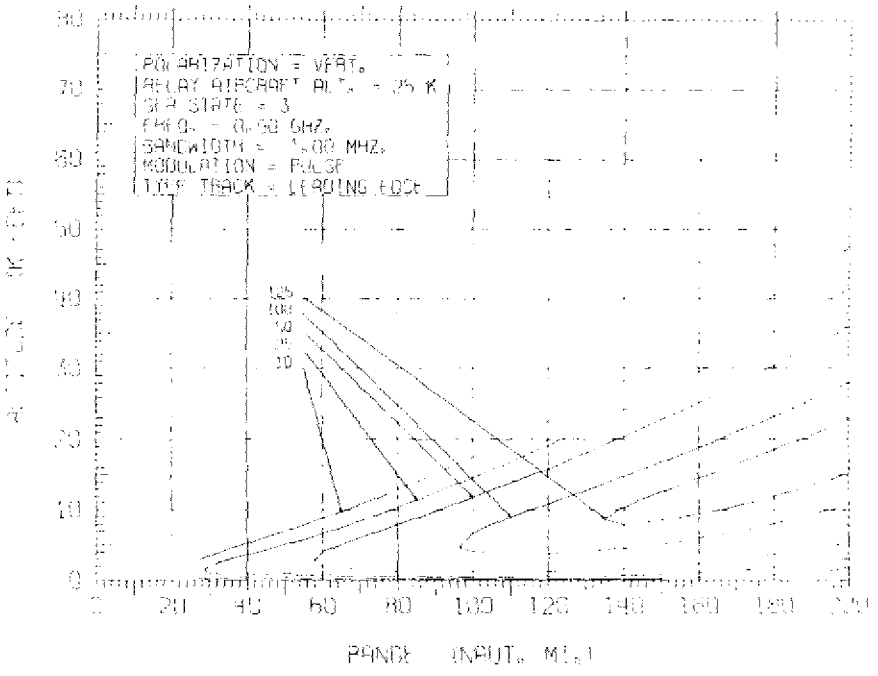

Fig. 9 — Contours of rms range errors

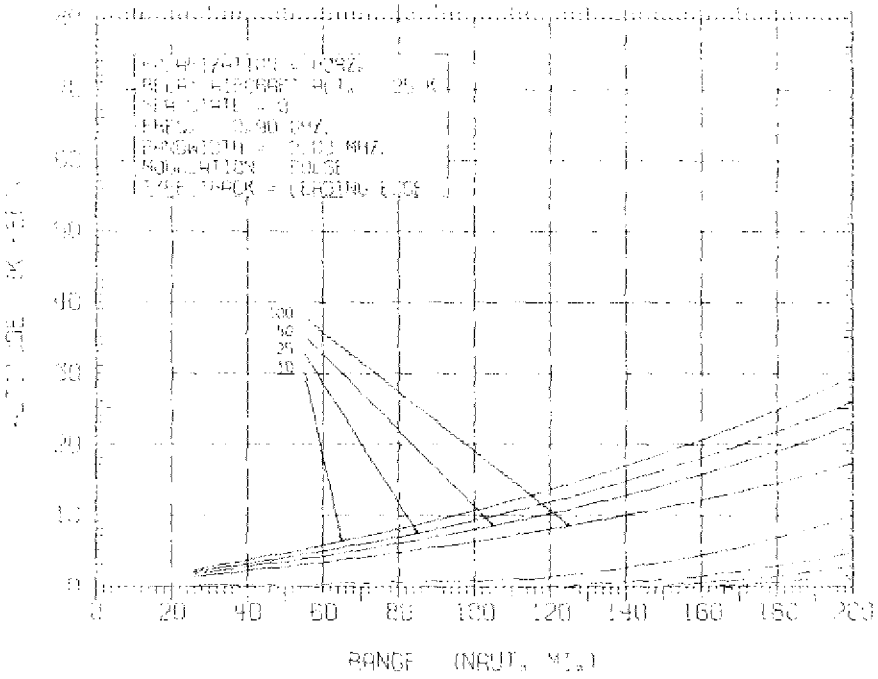

Fig. 10 — Contours of rms range errors

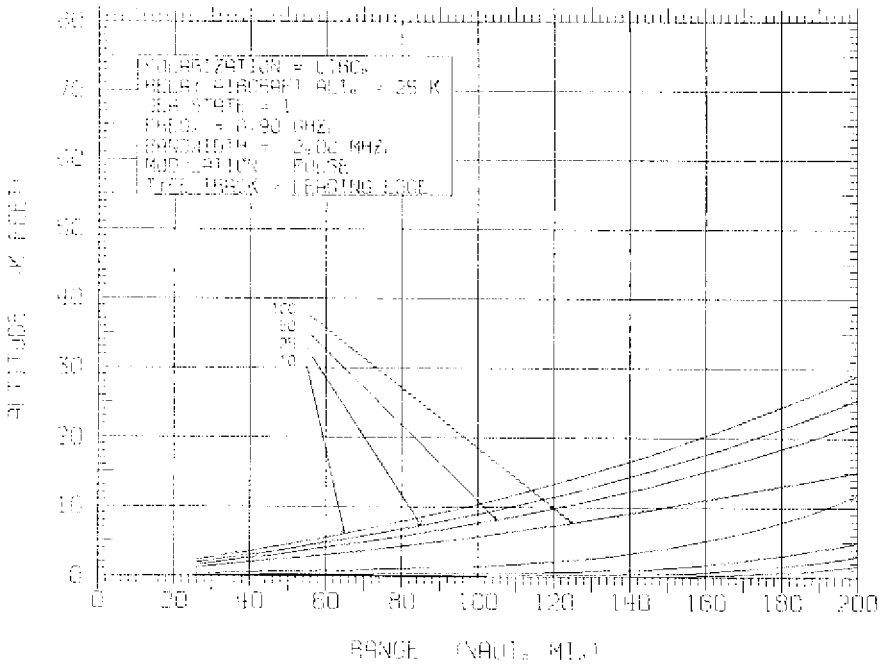

Fig. 11 — Contours of rms range errors

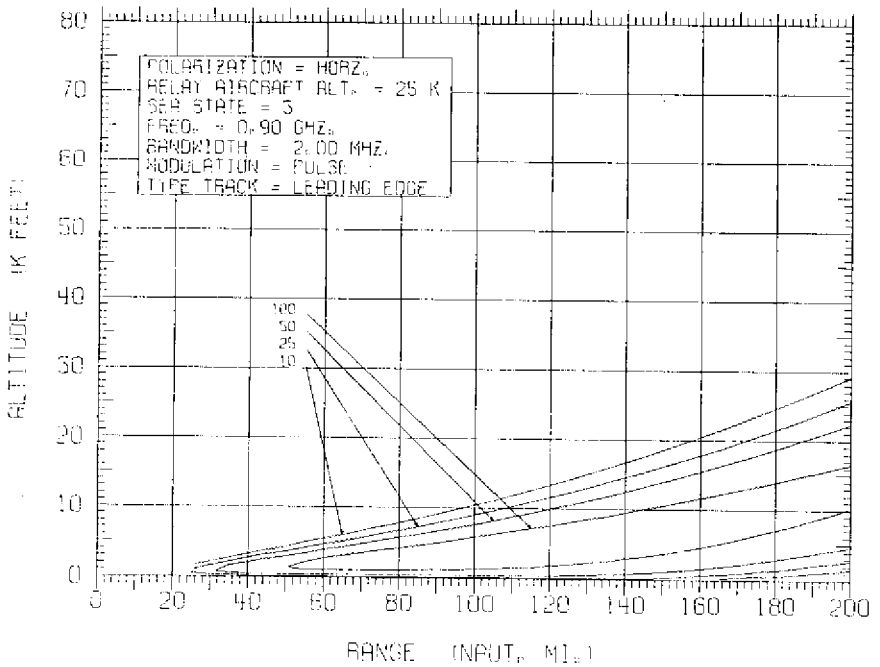

Fig. 12 — Contours of rms range errors

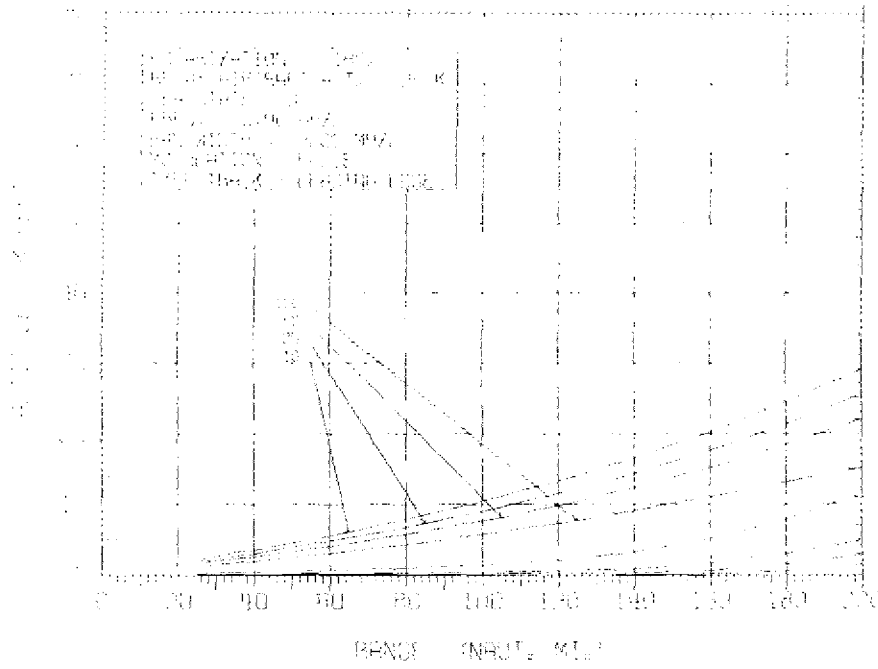

Fig. 13 — Contours of rms range errors

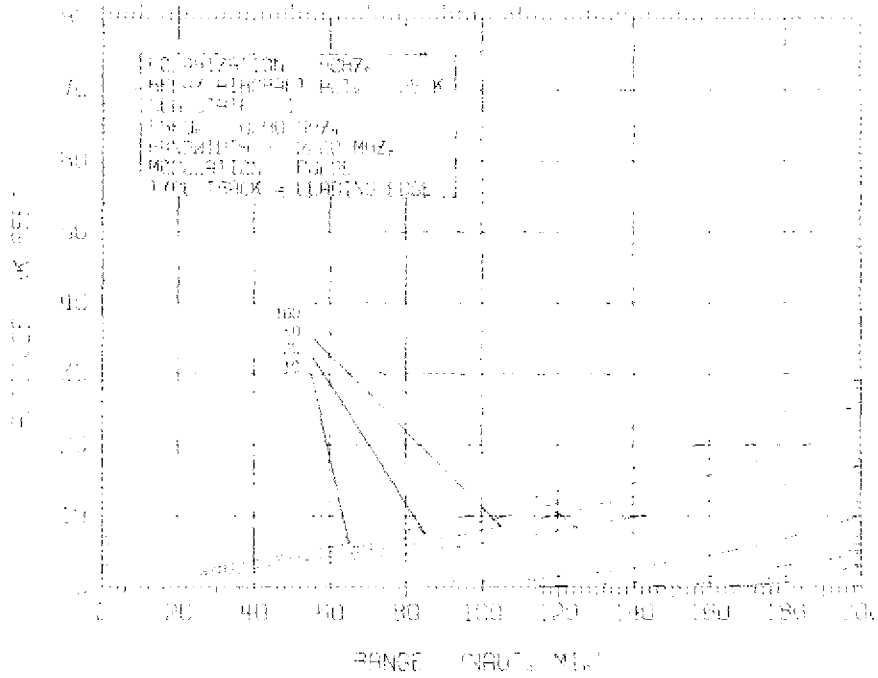

Fig. 14 — Contours of rms range errors

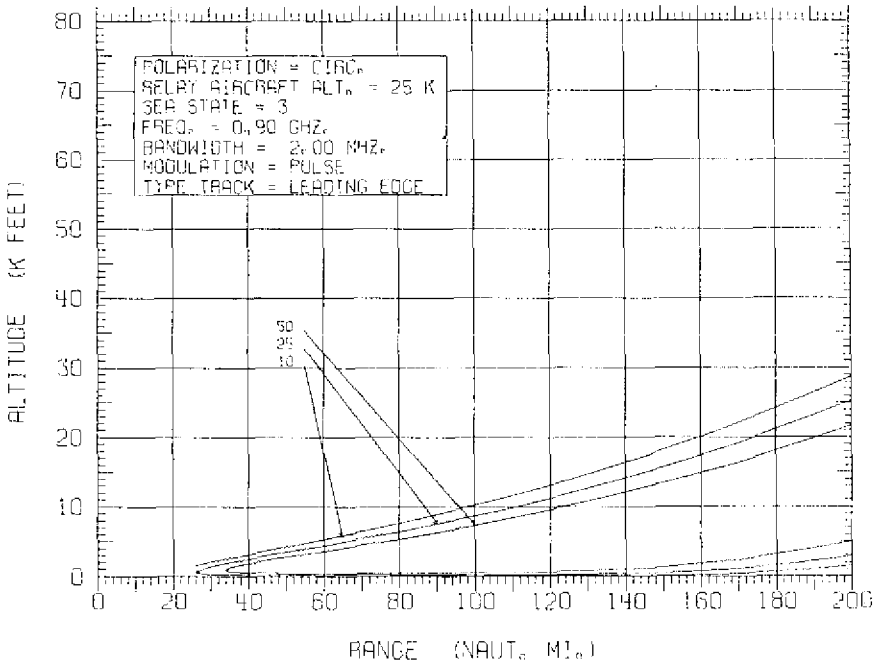

Fig. 15 — Contours of rms range errors

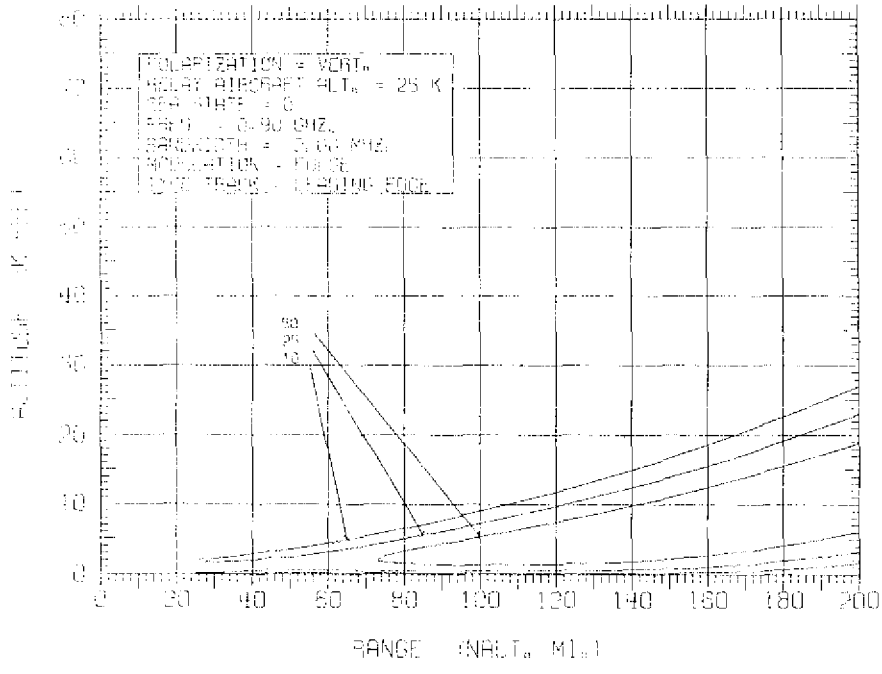

Fig. 16 — Contours of rms range errors

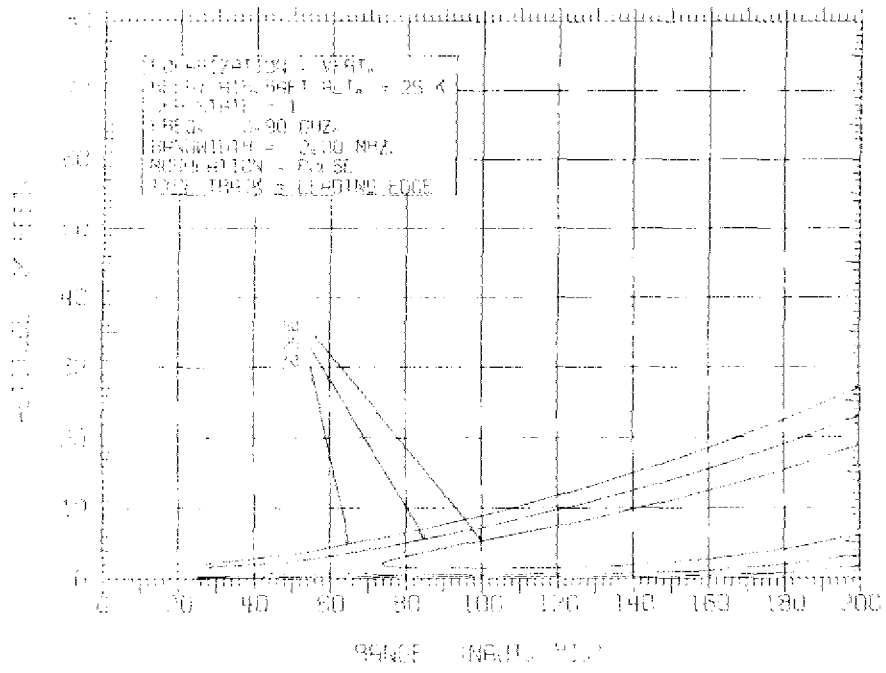

Fig. 17 — Contours of rms range errors

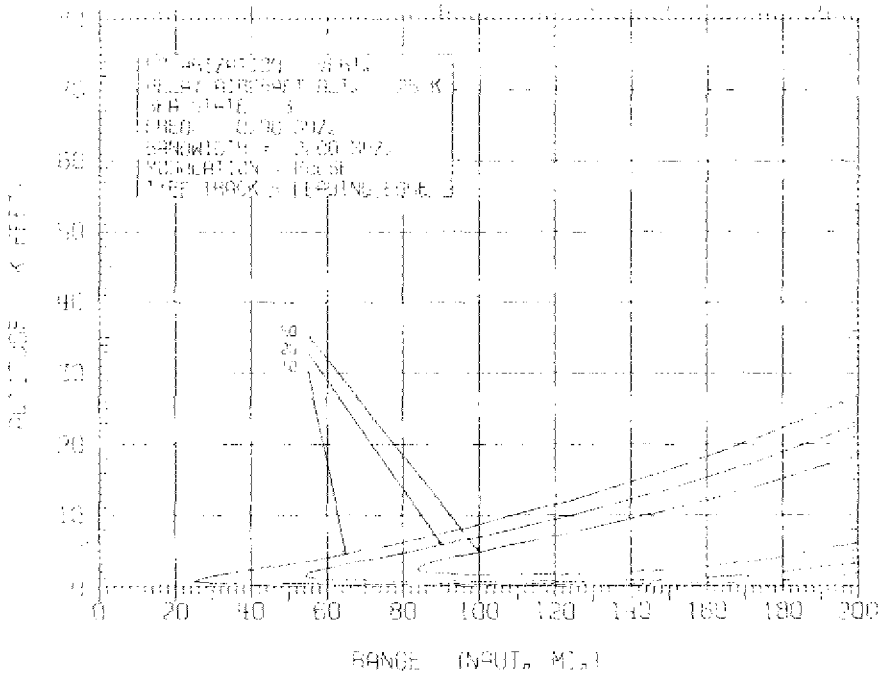

Fig. 18 — Contours of rms range errors

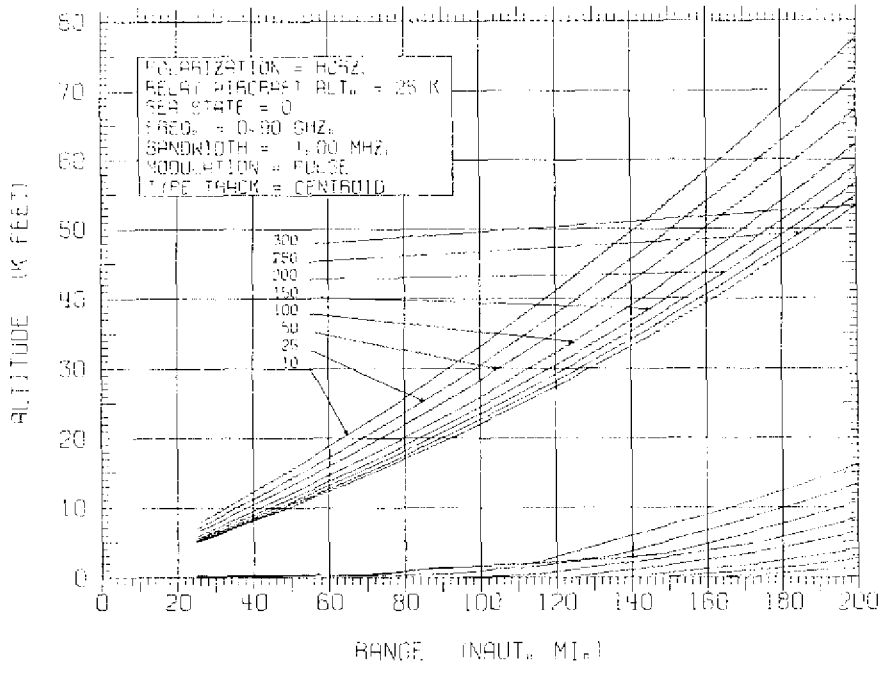

Fig. 19 — Contours of rms range errors

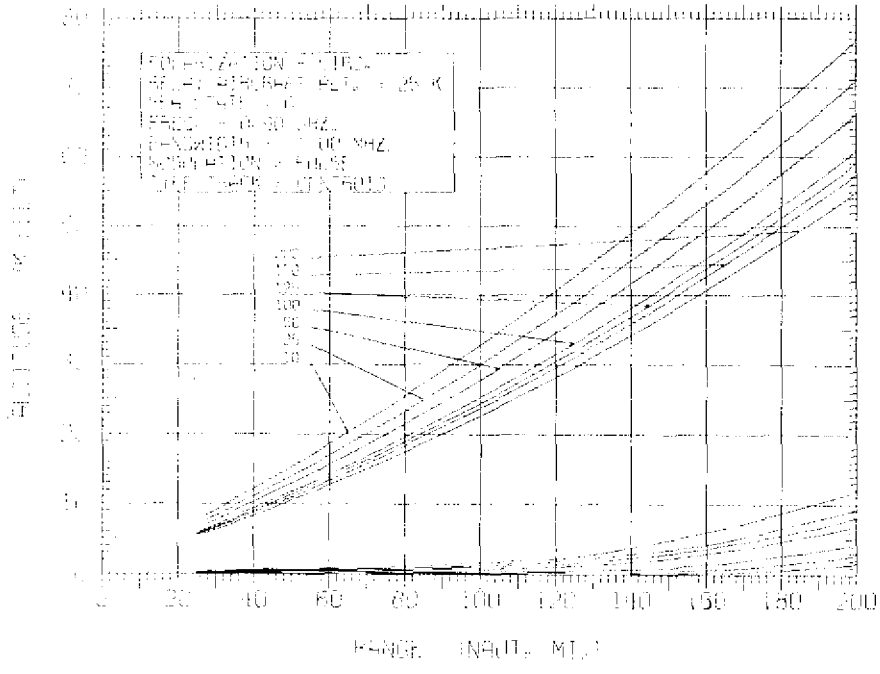

Fig. 20 — Contours of rms range errors

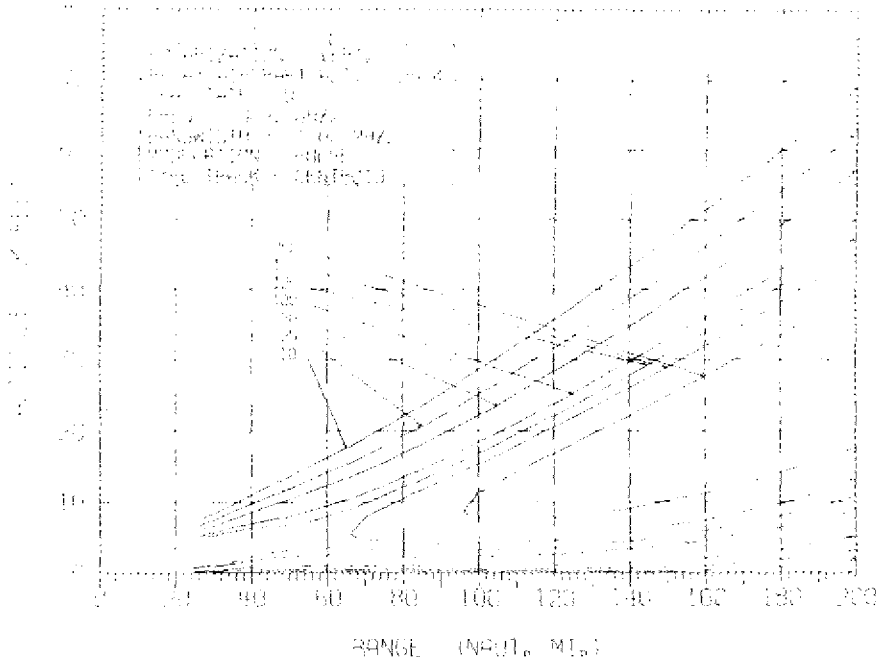

Fig. 21 — Contours of rms range errors

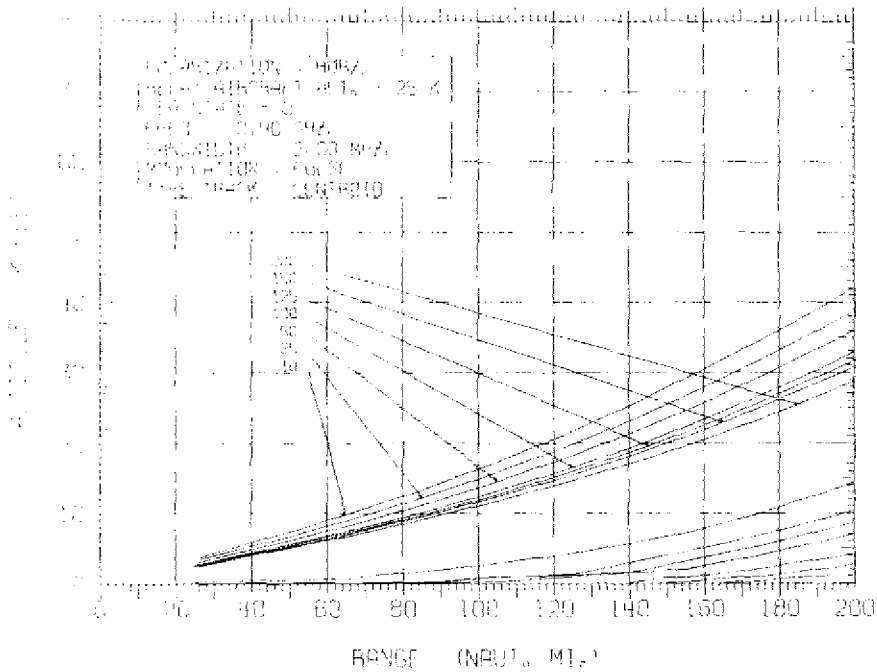

Fig. 22 — Contours of rms range errors

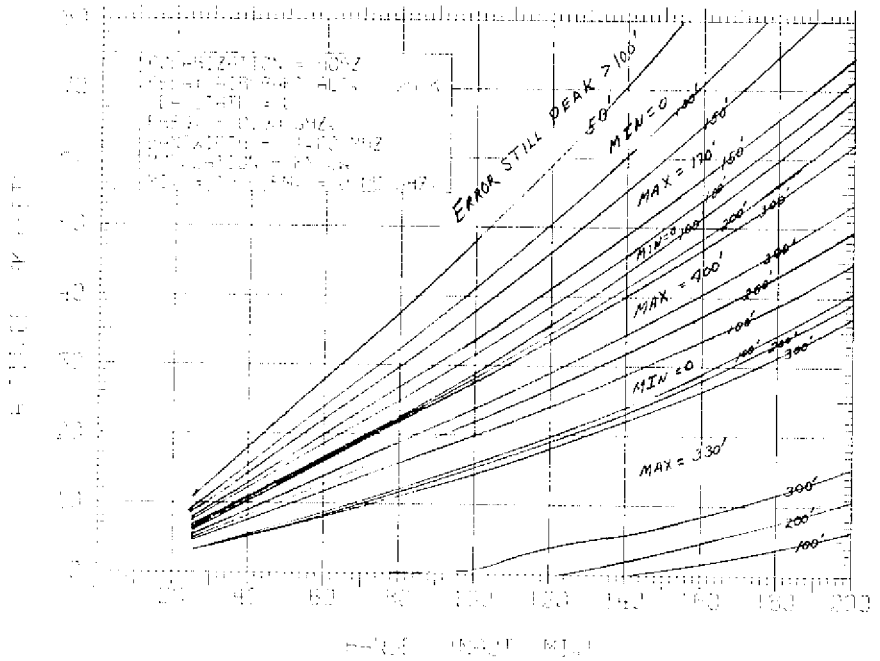

Fig. 23 — Contours of rms range errors

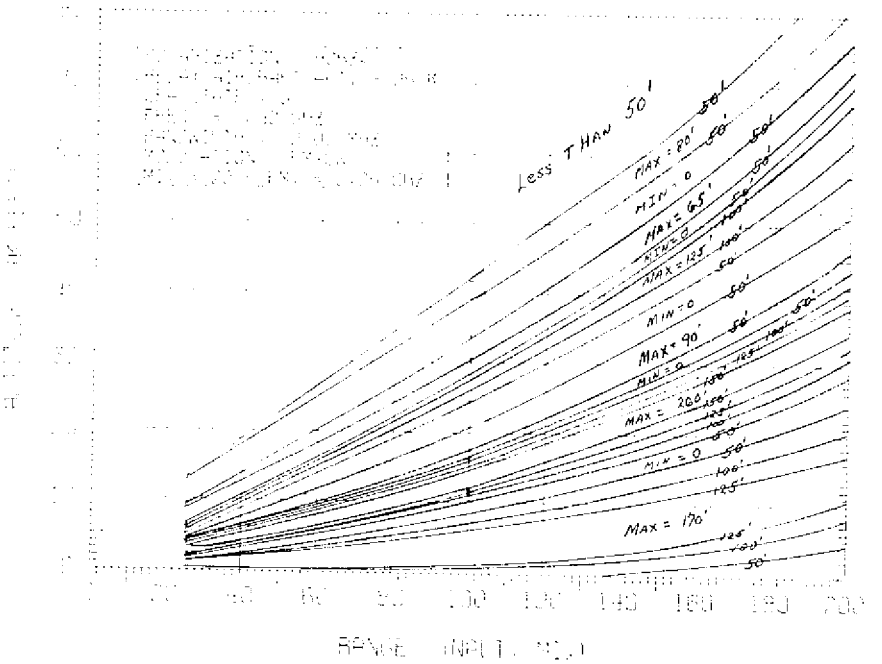

Fig. 24 — Contours of rms range errors

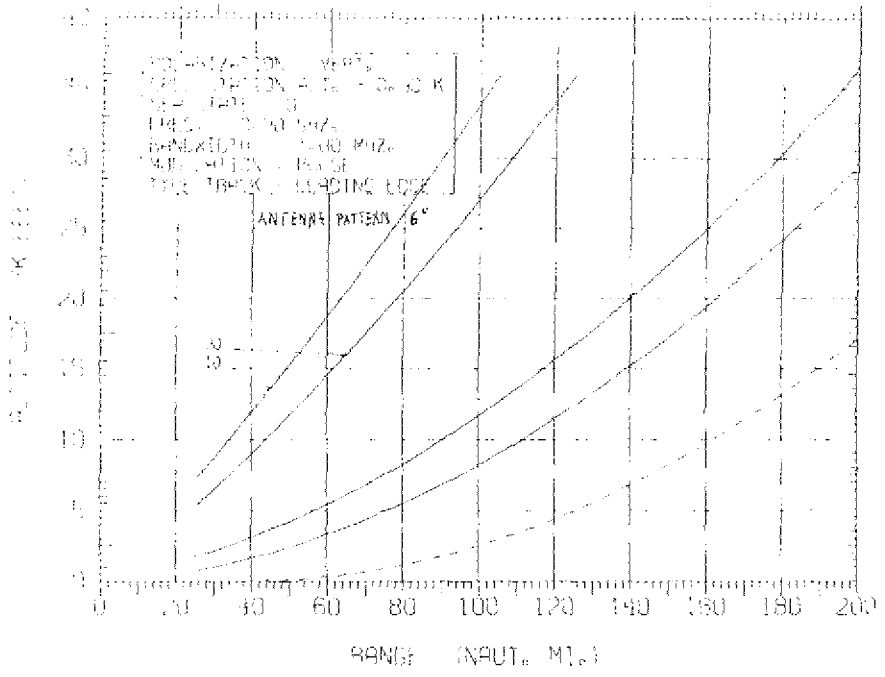

Fig. 25 — Contours of rms range errors

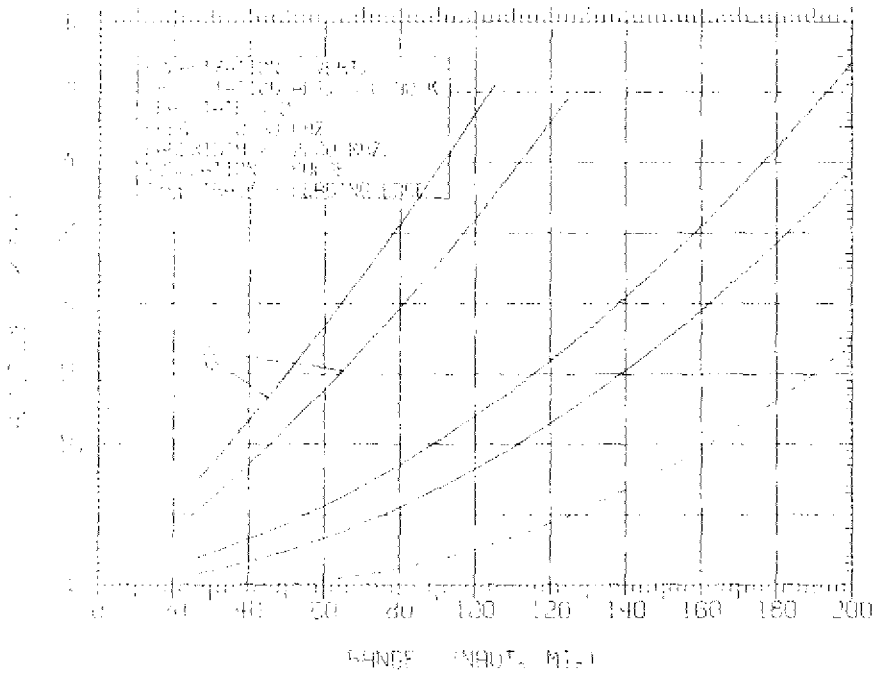

Fig. 26 — Contours of rms range errors

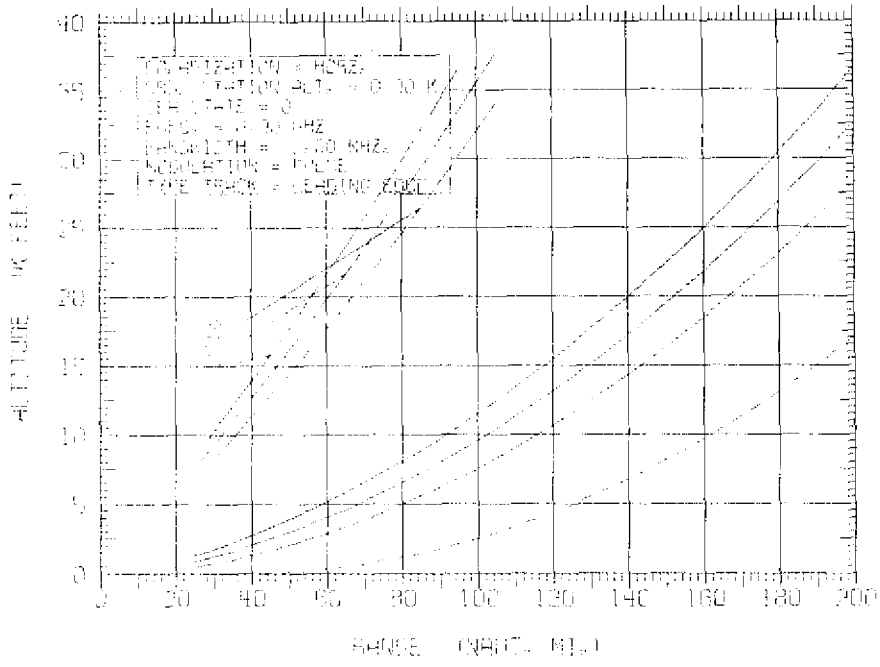

Fig. 27 — Contours of rms range errors

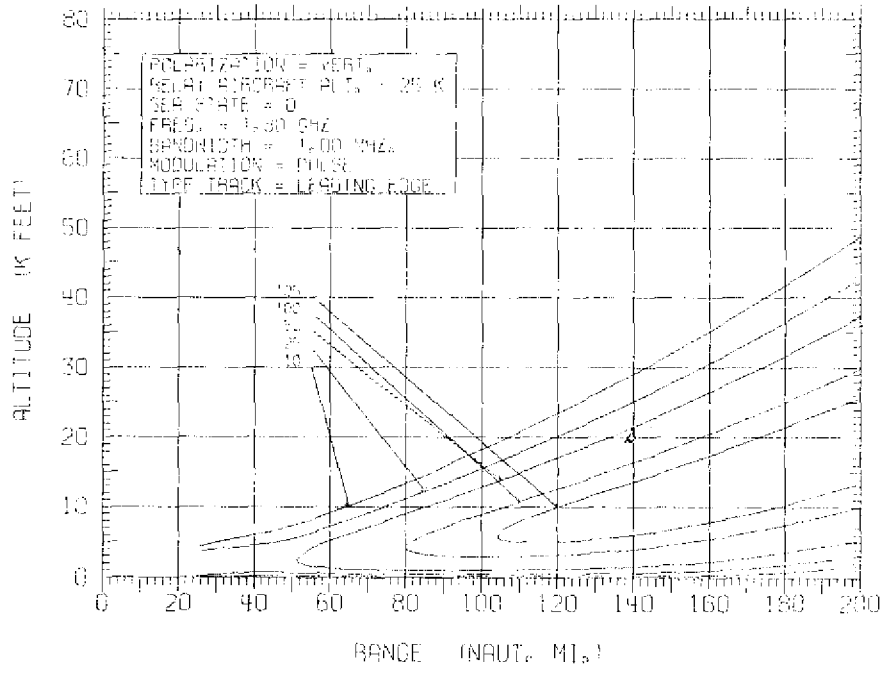

Fig. 28 — Contours of rms range errors

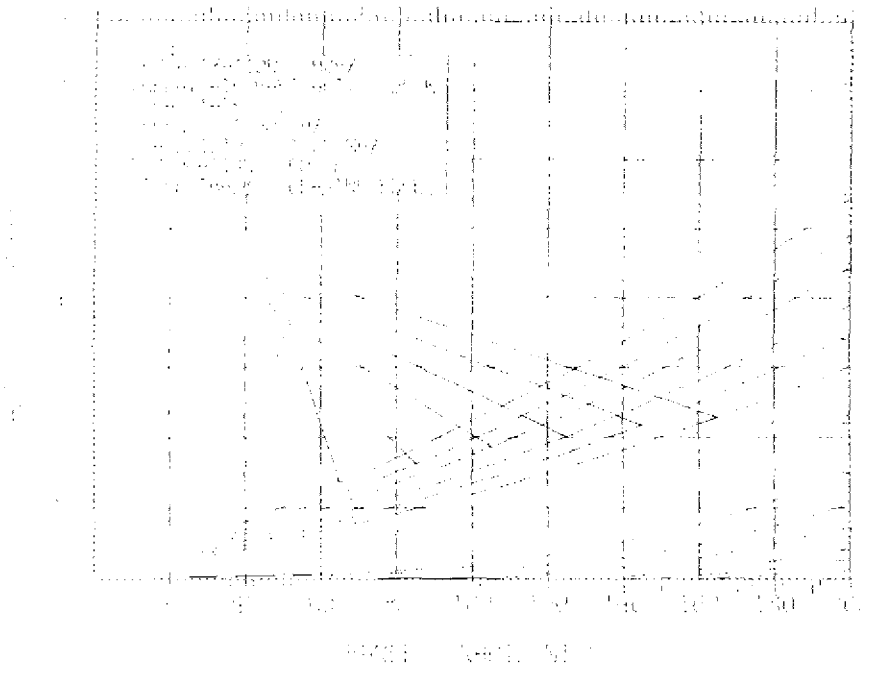

Fig. 29 — Contours of rms range errors

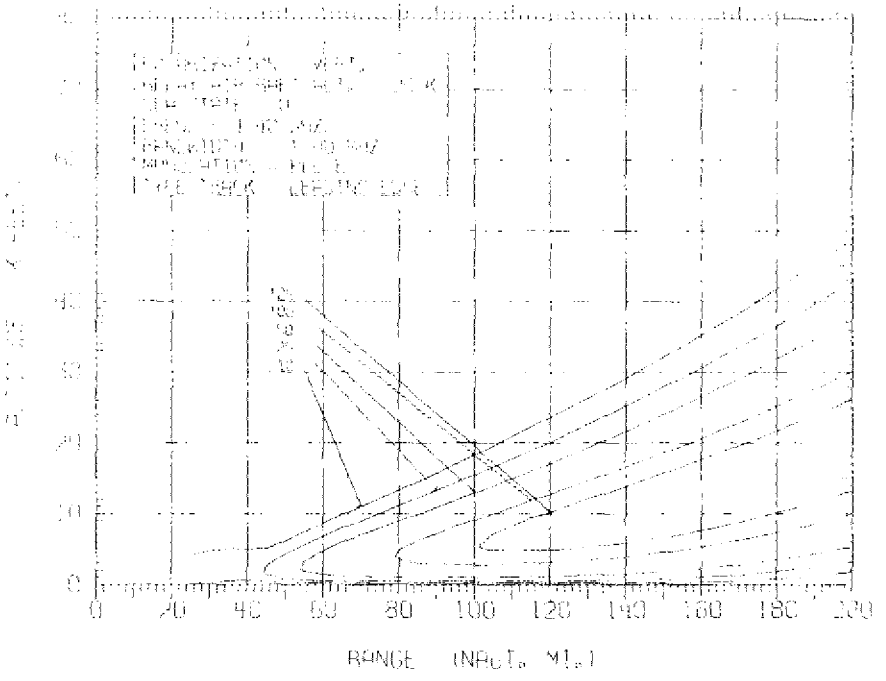

Fig. 30 — Contours of rms range errors

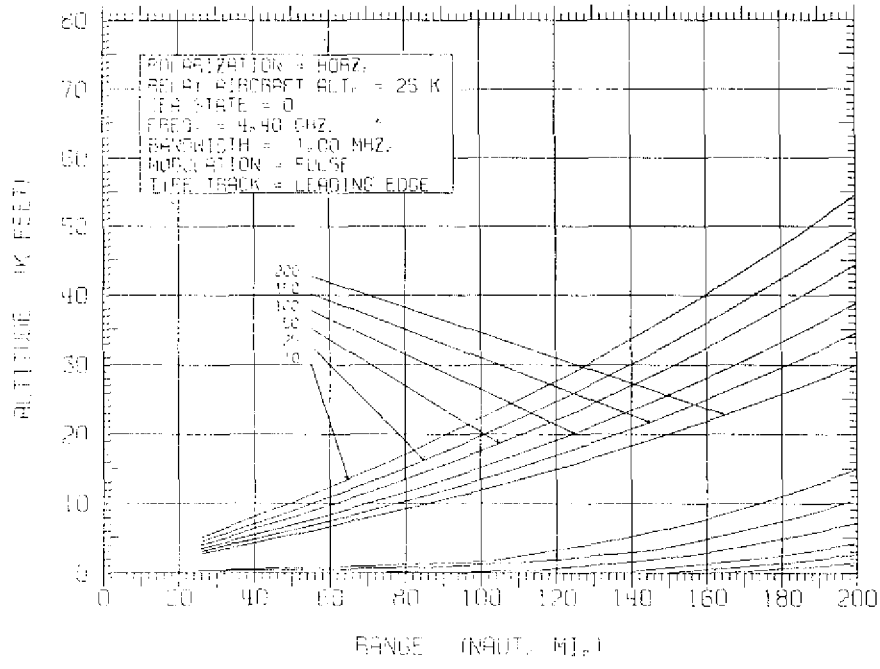

Fig. 31 — Contours of rms range errors

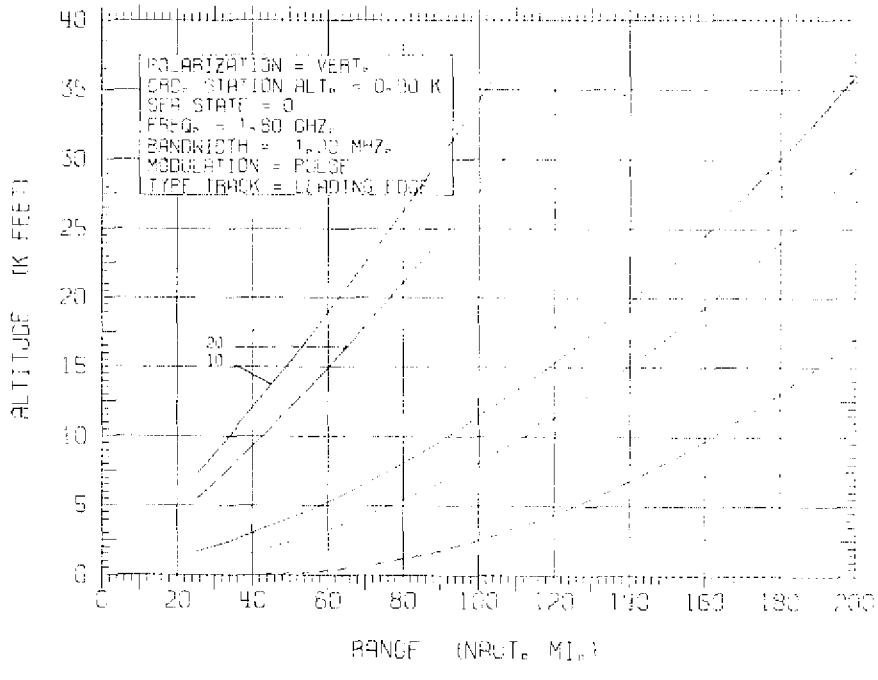

Fig. 32 — Contours of rms range errors

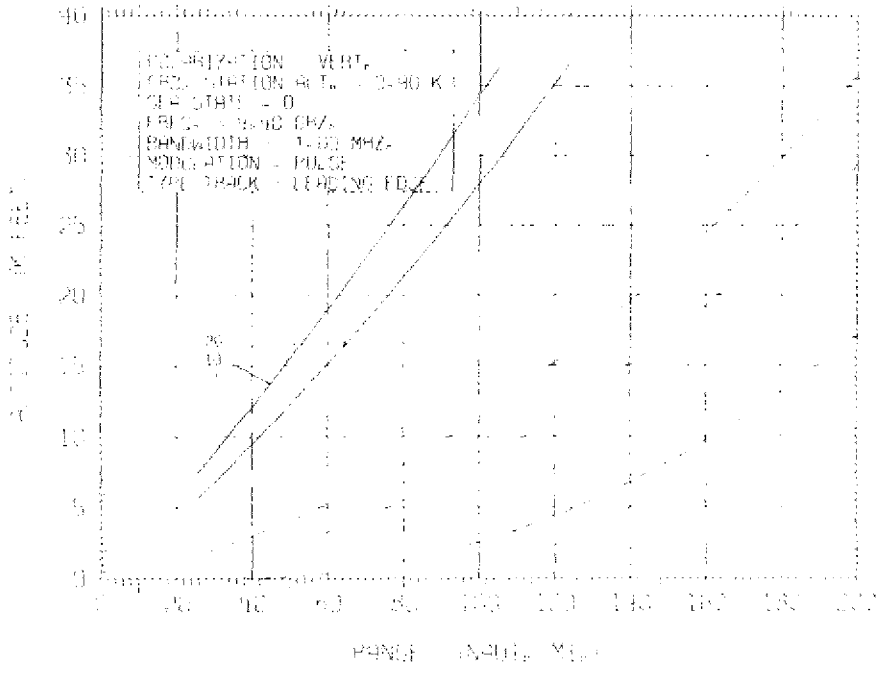

Fig. 33 — Contours of rms range errors

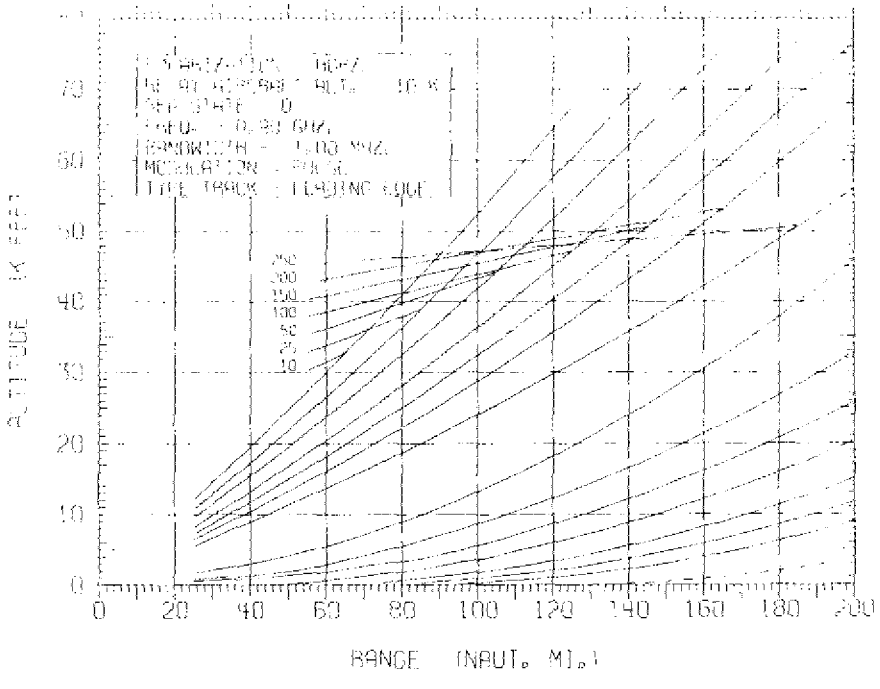

Fig. 34 — Contours of rms range errors

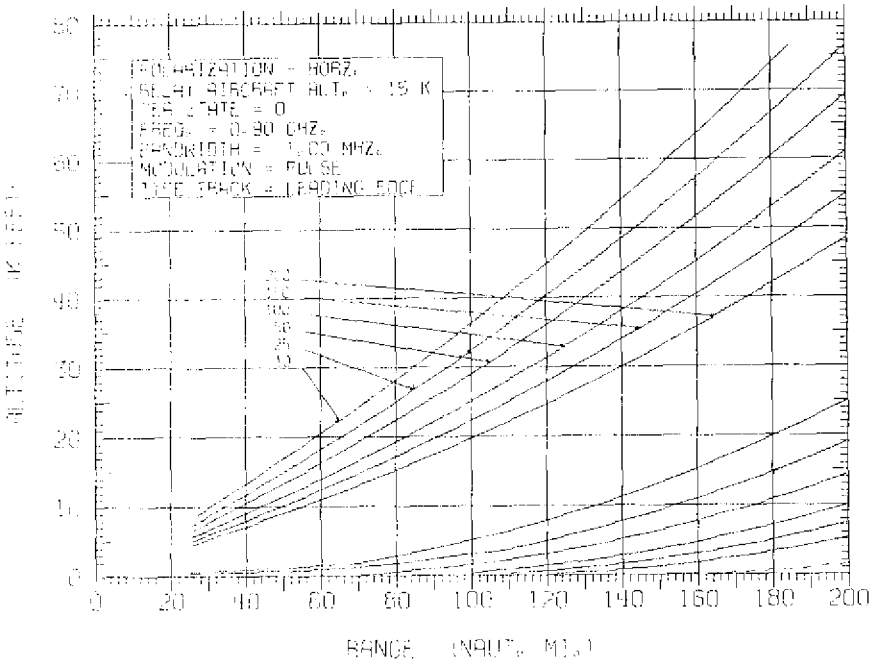

Fig. 35 — Contours of rms range errors

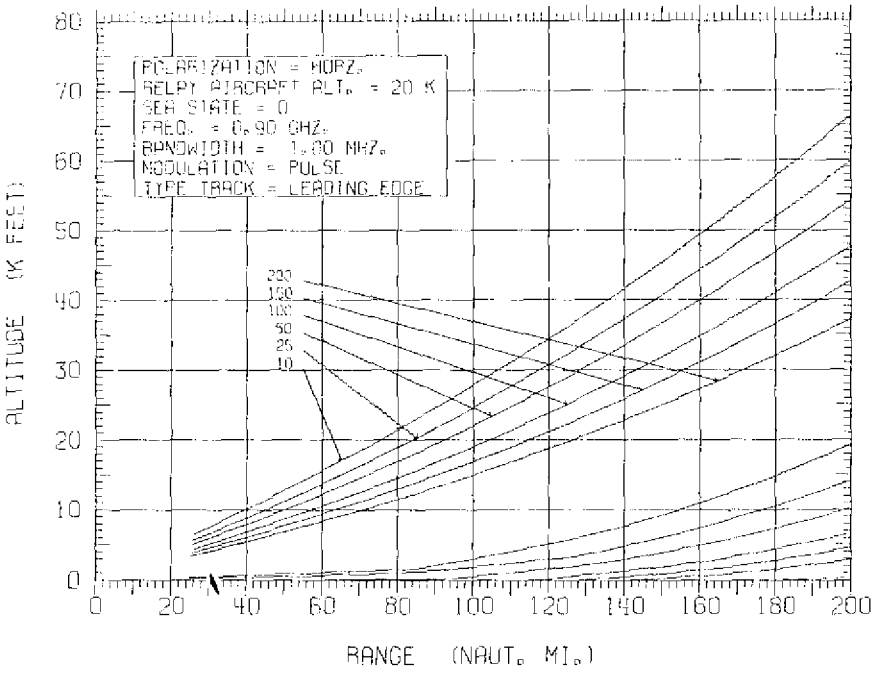

Fig. 36 — Contours of rms range errors

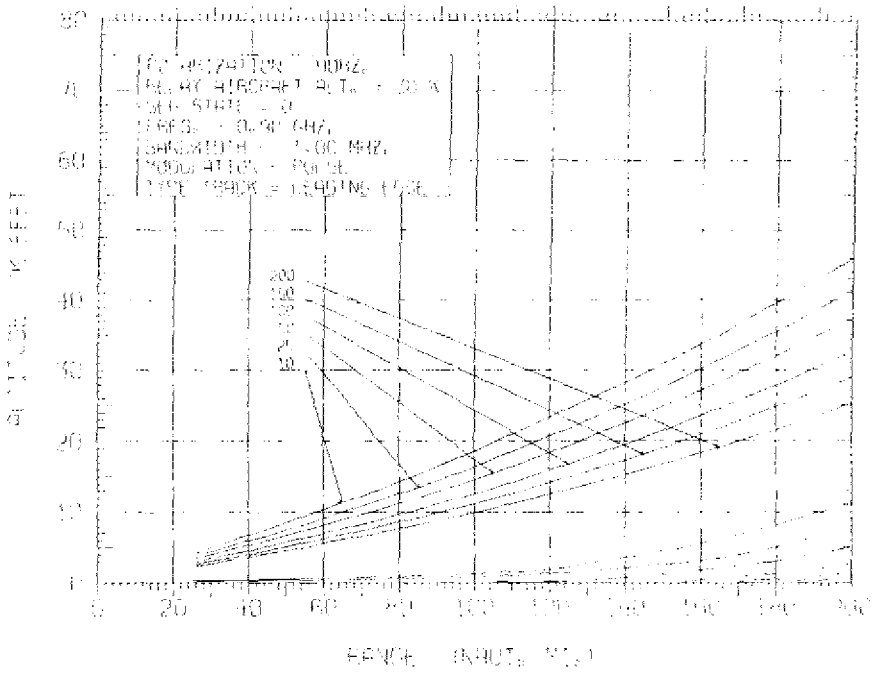

Fig. 37 — Contours of rms range errors

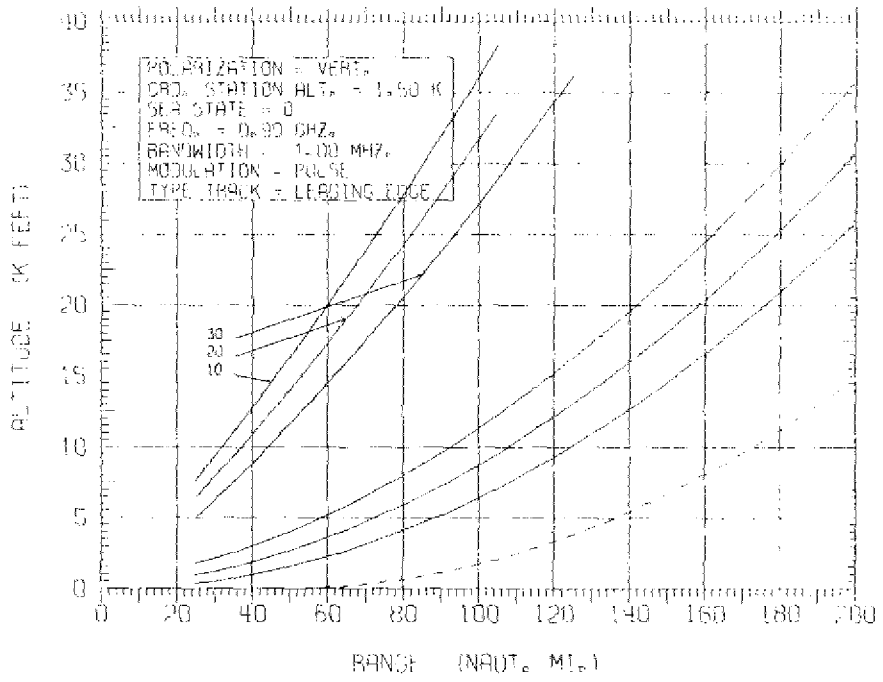

Fig. 38 — Contours of rms range errors

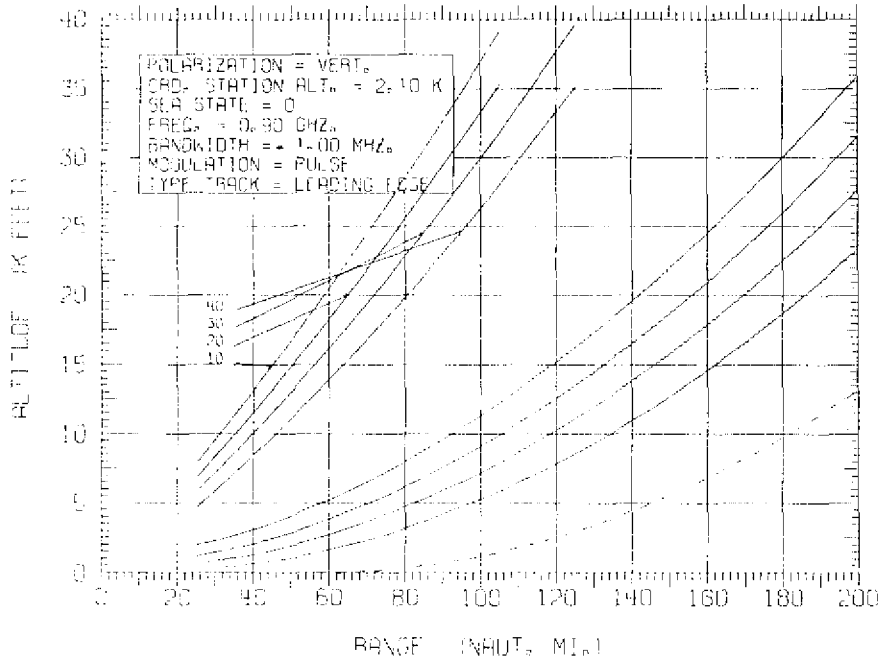

Fig. 39 — Contours of rms range errors

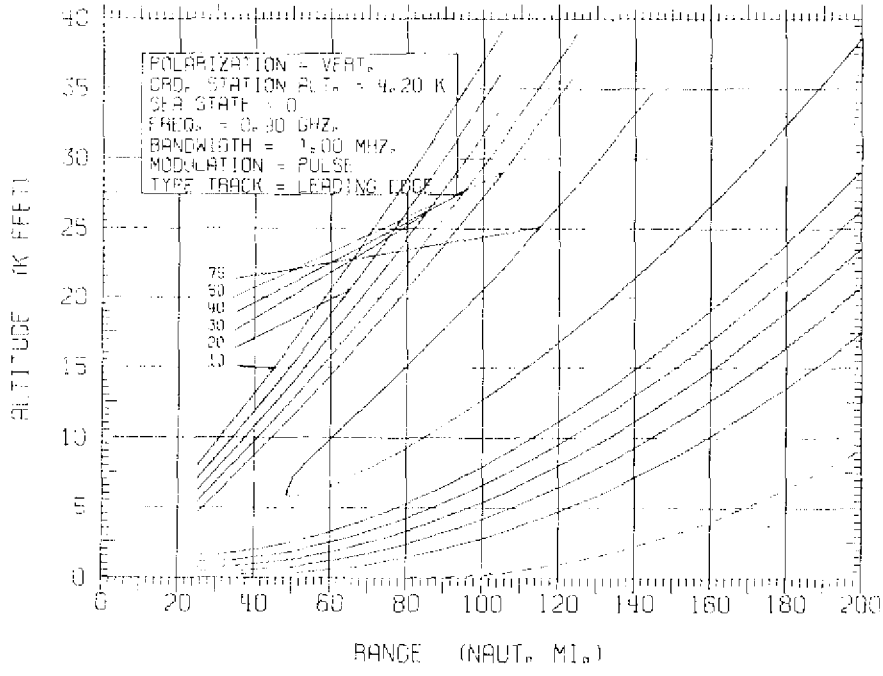

Fig. 40 — Contours of rms range errors

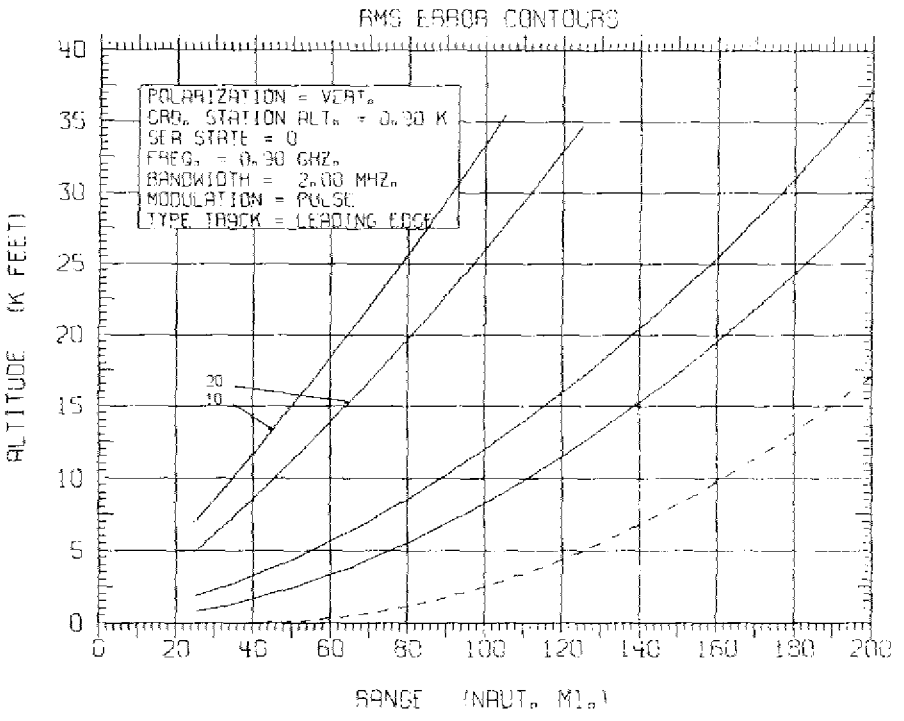

Fig. 41 — Contours of rms range errors

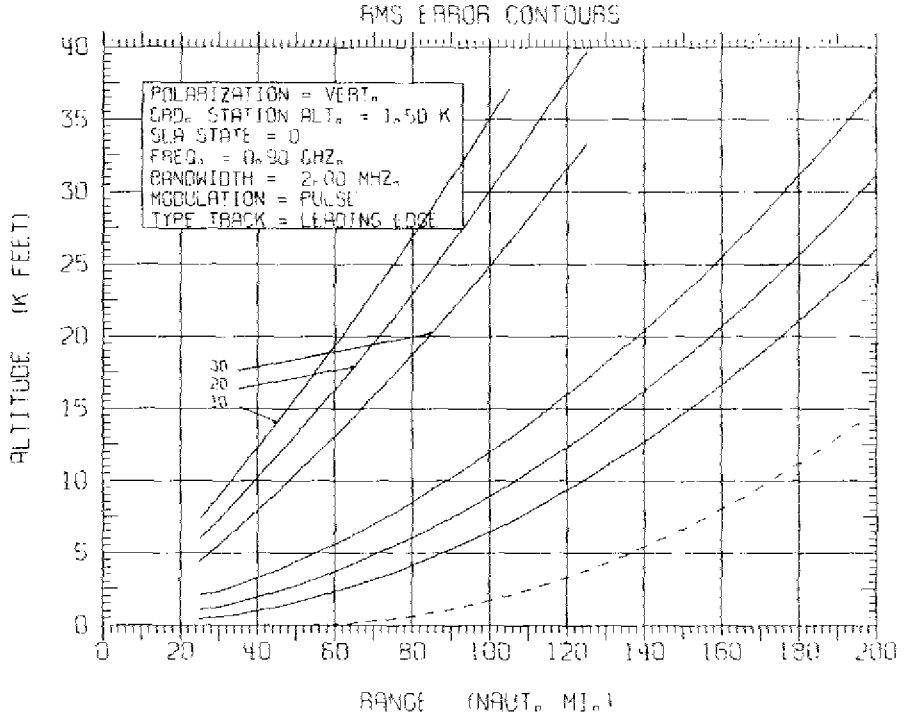

Fig. 42 — Contours of rms range errors

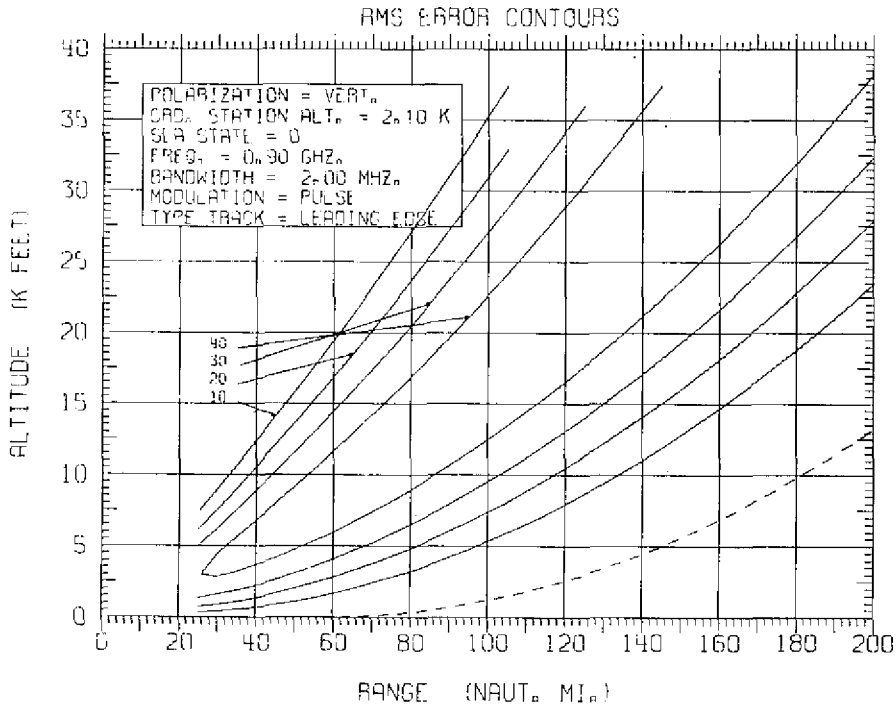

Fig. 43 — Contours of rms range errors

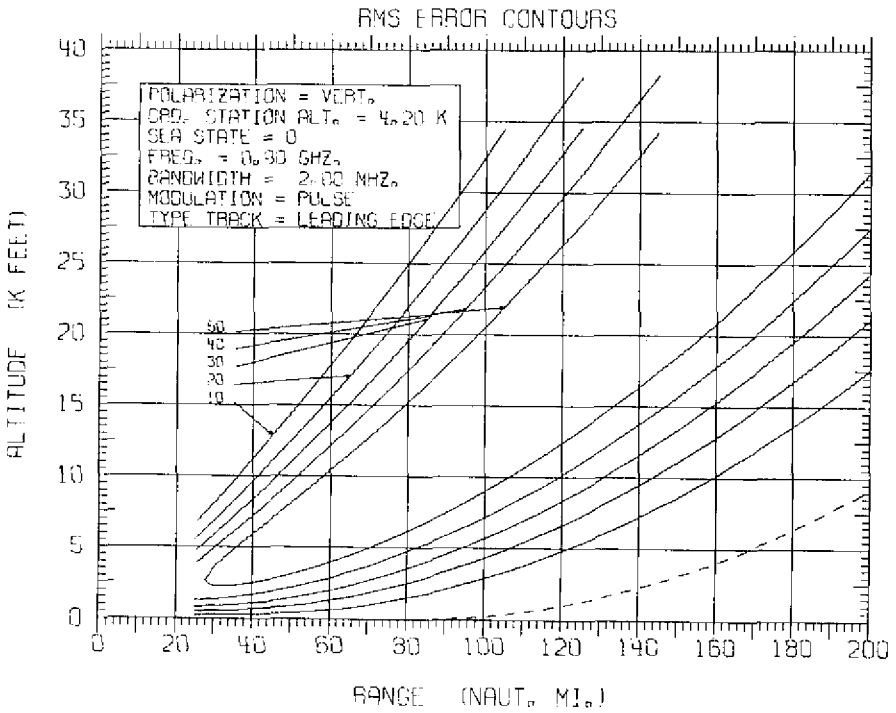

Fig. 44 — Contours of rms range errors

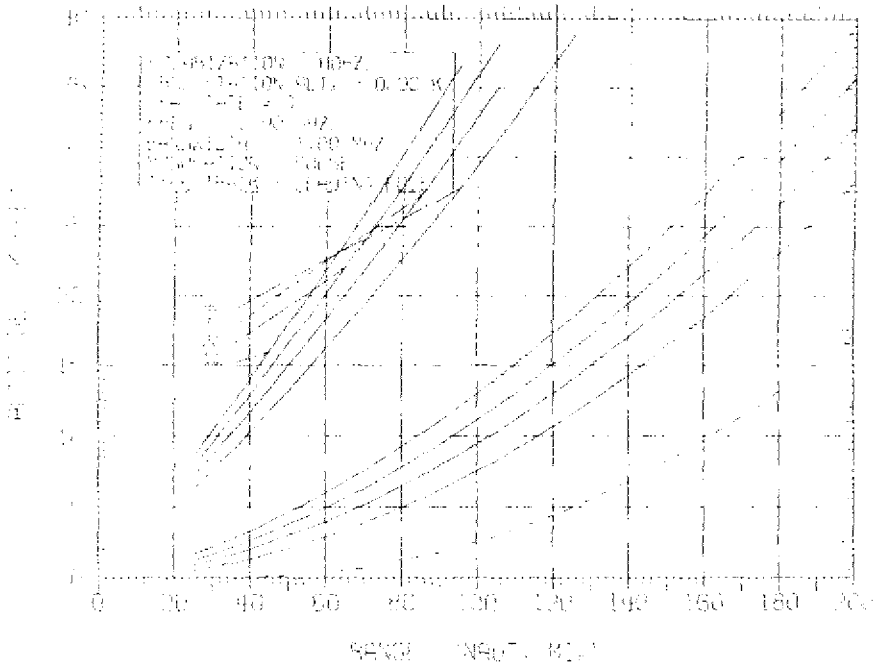

Fig. 45 — Contours of rms range errors

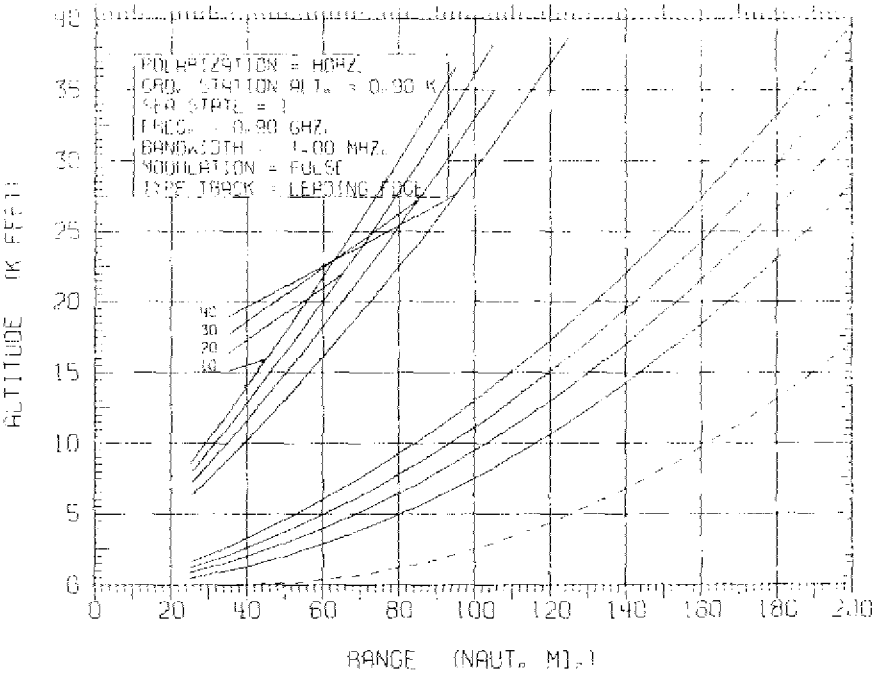

Fig. 46 — Contours of rms range errors

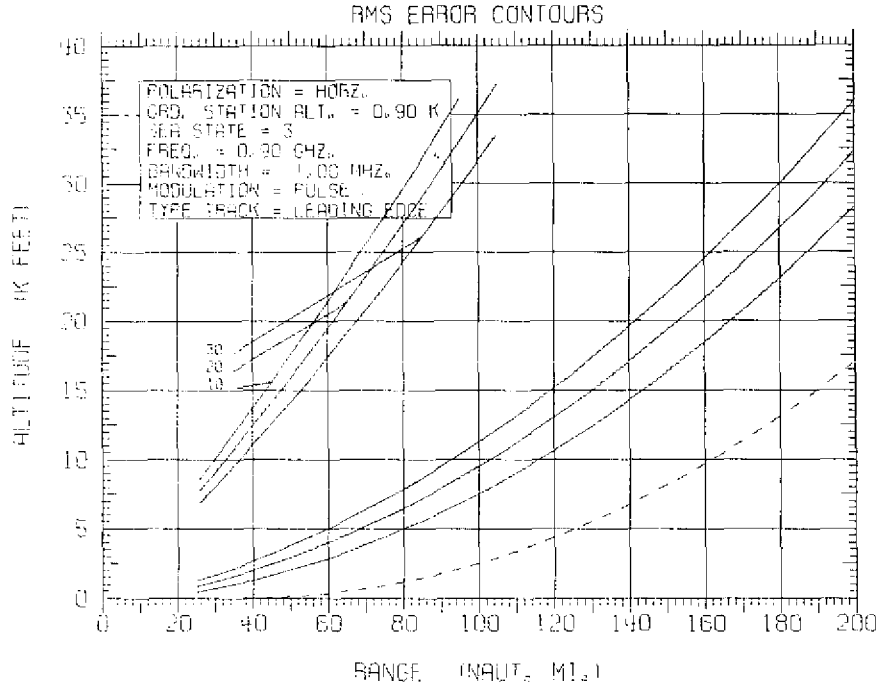

Fig. 47 — Contours of rms range errors

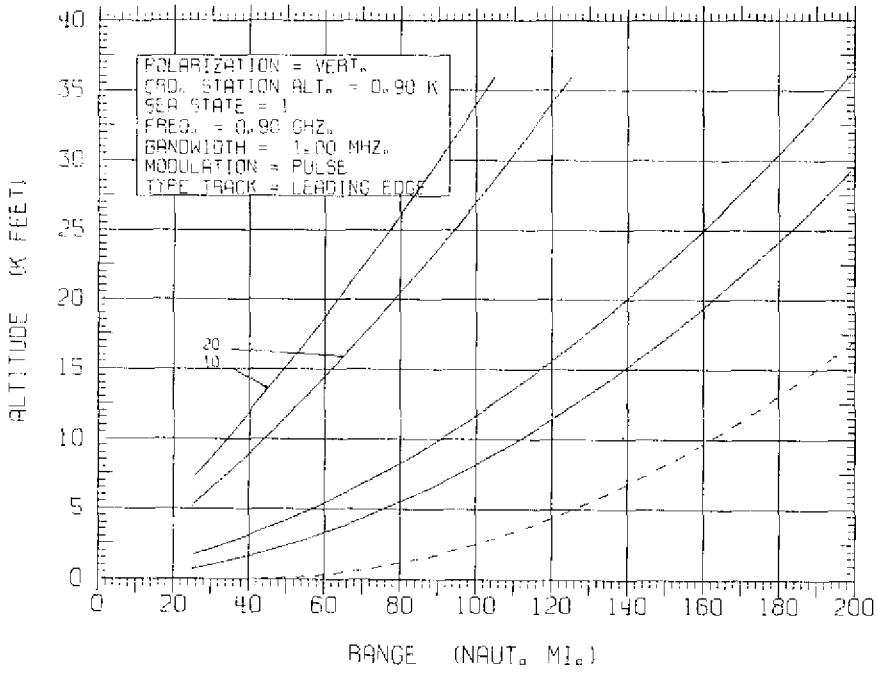

Fig. 48 — Contours of rms range errors

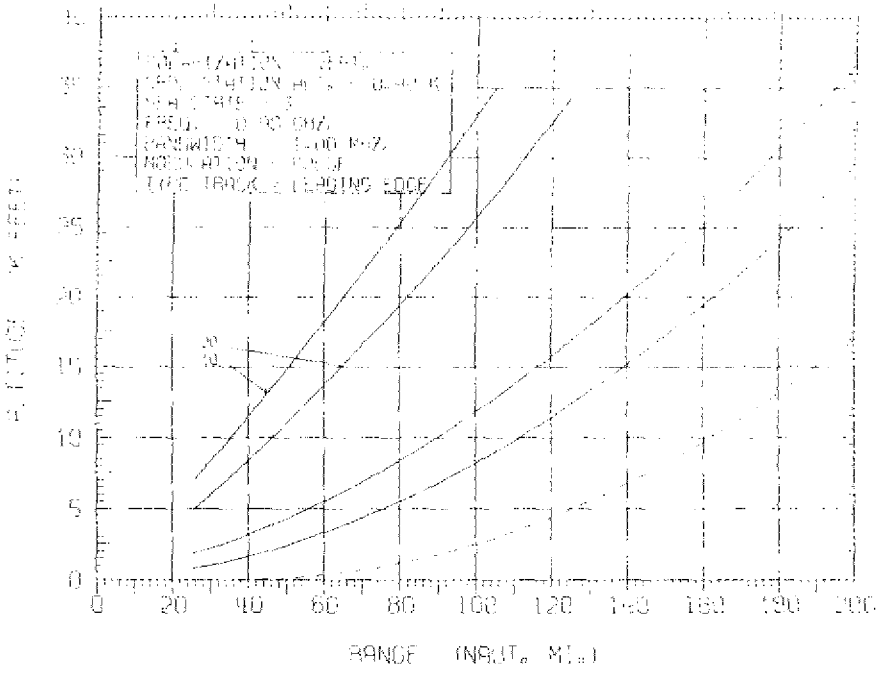

Fig. 49 — Contours of rms range errors

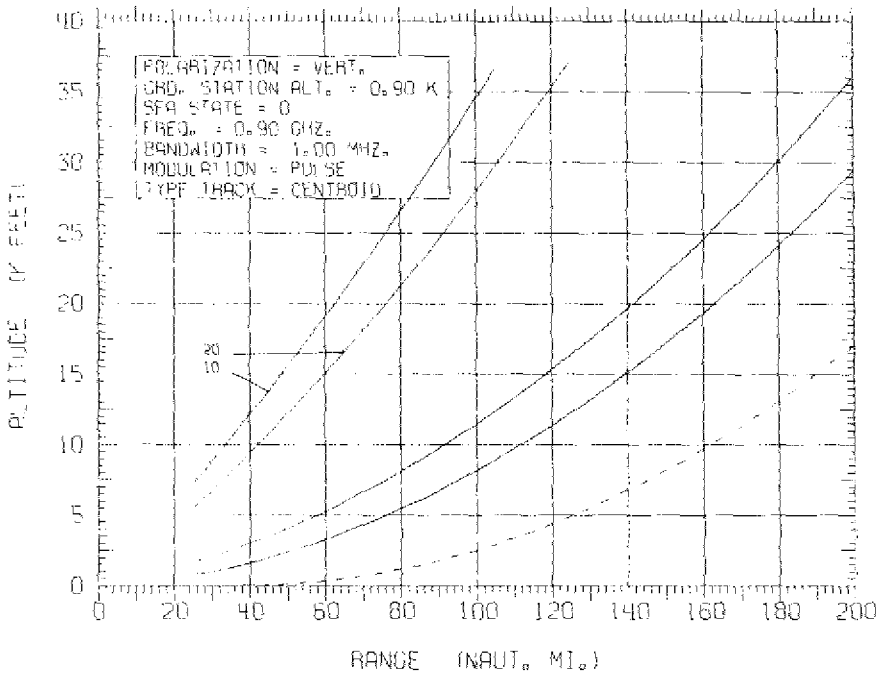

Fig. 50 — Contours of rms range errors

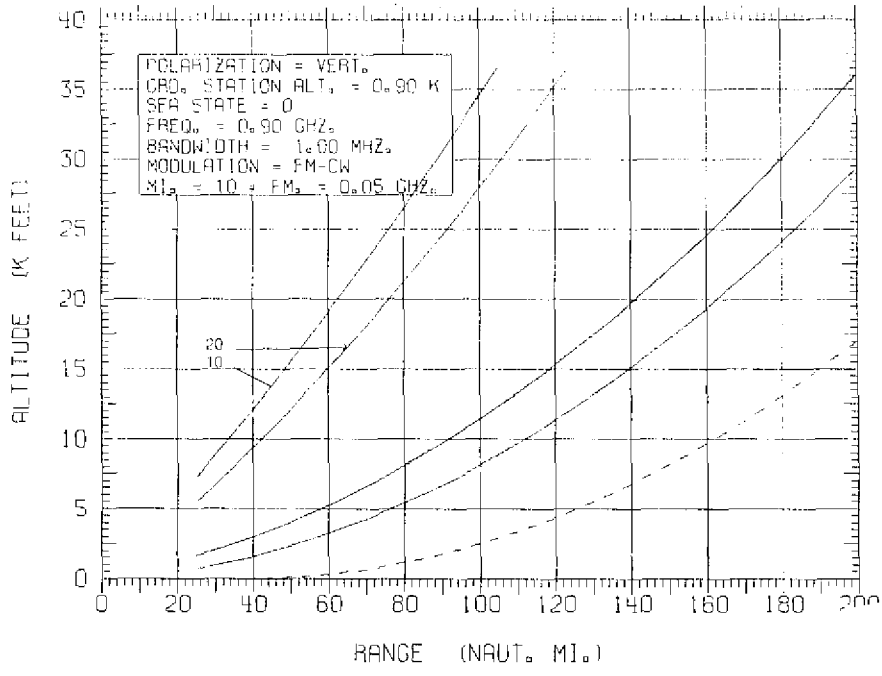

Fig. 51 — Contours of rms range errors

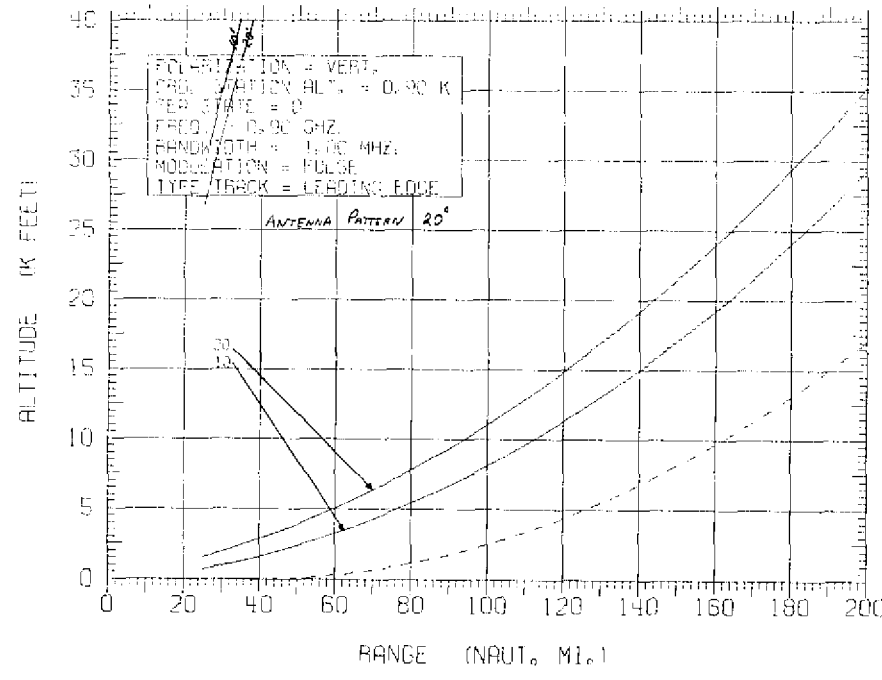

Fig. 52 — Contours of rms range errors

System Bandwidth

Table 1 lists the plots chosen to study the effects of system bandwidth. The choice of system bandwidth has a major impact on the amplitude of the multipath errors for the link between one of the relay aircraft and the tracked object. When the bandwidth is increased from 1 MHz to 2 MHz, the area bounded by each contour is reduced by approximately half. The maximum value of the errors (peak or rms) is also approximately inversely proportional to bandwidth for the range of values of interest.

Table 1
Plots Chosen to Study the Effects of System Bandwidth

Figure	System Bandwidth (MHz)	RF Freq. (GHz)	Relay-Aircraft Altitude (kft)	Ground-Station Altitude (kft)	Polarization	Sea State	Modulation Technique	Tracking Technique	Ground Station-Antenna Beamwidth (deg)
1	1.00	0.90	25	NA*	Horiz.	0	Pulse	Leading edge	NA
2	1.00	0.90	25	NA*	Horiz.	1	Pulse	Leading edge	NA
3	1.00	0.90	25	NA*	Horiz.	3	Pulse	Leading edge	NA
4	1.00	0.90	25	NA*	Circ.	0	Pulse	Leading edge	NA
5	1.00	0.90	25	NA*	Circ.	1	Pulse	Leading edge	NA
6	1.00	0.90	25	NA*	Circ.	3	Pulse	Leading edge	NA
7	1.00	0.90	25	NA*	Vert.	0	Pulse	Leading edge	NA
8	1.00	0.90	25	NA*	Vert.	1	Pulse	Leading edge	NA
9	1.00	0.90	25	NA*	Vert.	3	Pulse	Leading edge	NA
10	2.00	0.90	25	NA*	Horiz.	0	Pulse	Leading edge	NA
11	2.00	0.90	25	NA*	Horiz.	1	Pulse	Leading edge	NA
12	2.00	0.90	25	NA*	Horiz.	3	Pulse	Leading edge	NA
13	2.00	0.90	25	NA*	Circ.	0	Pulse	Leading edge	NA
14	2.00	0.90	25	NA*	Circ.	1	Pulse	Leading edge	NA
15	2.00	0.90	25	NA*	Circ.	3	Pulse	Leading edge	NA
16	2.00	0.90	25	NA*	Vert.	0	Pulse	Leading edge	NA
17	2.00	0.90	25	NA*	Vert.	1	Pulse	Leading edge	NA
18	2.00	0.90	25	NA*	Vert.	3	Pulse	Leading edge	NA
19	1.00	0.90	25	NA*	Horiz.	0	Pulse	Centroid	NA
20	1.00	0.90	25	NA*	Circ.	0	Pulse	Centroid	NA
21	1.00	0.90	25	NA*	Vert.	0	Pulse	Centroid	NA
22	2.00	0.90	25	NA*	Horiz.	0	Pulse	Centroid	NA
23	1.00	0.90	25	NA*	Horiz.	0	FM/CW	NA	NA
24	2.00	0.90	25	NA*	Horiz.	0	FM/CW	NA	NA
25	1.00	0.90	NA	0.90	Vert.	0	Pulse	Leading edge	6
26	2.00	0.90	NA	0.90	Vert.	0	Pulse	Leading edge	6
27	2.00	0.90	NA	0.90	Horiz.	0	Pulse	Leading edge	6

*Not applicable to the case under consideration.

In the link from the ground station to the relay aircraft however the increase in bandwidth does not produce a major reduction in the errors. This is because the geometry is such that the path-length differences from the ground station to the relay aircraft are smaller than between the relay aircraft and the tracked object. Small path-length differences do not allow the 0.5- and 1-microsecond pulses to resolve the direct and indirect

signals. A much larger bandwidth than 2 MHz would be required to obtain resolution and reduce the multipath errors to zero. The small path-length differences do however keep the magnitude of the errors much lower than those observed in the airborne link. The choice of bandwidth will therefore be governed by the airborne link and should be as large as is possible.

RF Frequency

Table 2 lists the plots chosen to study the effects of RF frequency. The choice of RF frequency has only a minor effect on the area enclosed by various contours, but it does have a major effect on the cyclic nature of the multipath error. For a given target trajectory the rate at which the error fluctuates is directly proportional to the RF frequency. For an RF frequency of 4.4 GHz, the same amount of averaging can be accomplished in about 1/5 the time required at 0.9 GHz. For certain target trajectories the errors will fluctuate slowly for any of the RF frequencies considered here. This is true for low-altitude horizontal trajectories, which is an important case in EATS operations. The choice of RF frequency affects propagation losses, size, and weight of airborne equipment. Therefore, the tradeoffs between these factors and the possible time averaging must dictate the RF frequency.

Table 2
Plots Chosen to Study the Effects of RF Frequency

Figure	System Bandwidth (MHz)	RF Freq. (GHz)	Relay-Aircraft Altitude (kft)	Ground-Station Altitude (kft)	Polarization	Sea State	Modulation Technique	Tracking Technique	Ground Station-Antenna Beamwidth (deg)
7	1.00	0.90	25	NA	Vert.	0	Pulse	Leading edge	NA
1	1.00	0.90	25	NA	Horiz.	0	Pulse	Leading edge	NA
28	1.00	1.80	25	NA	Vert.	0	Pulse	Leading edge	NA
29	1.00	1.80	25	NA	Horiz.	0	Pulse	Leading edge	NA
30	1.00	4.40	25	NA	Vert.	0	Pulse	Leading edge	NA
31	1.00	4.40	25	NA	Horiz.	0	Pulse	Leading edge	NA
25	1.00	0.90	NA	0.90	Vert.	0	Pulse	Leading edge	6
32	1.00	1.80	NA	0.90	Vert.	0	Pulse	Leading edge	6
33	1.00	4.40	NA	0.90	Vert.	0	Pulse	Leading edge	6

Relay-Aircraft Altitude and Ground-Station Altitude

Table 3 lists the plots chosen to study the effects of relay-aircraft altitude and ground-station altitude. The choice of a high relay-aircraft altitude can reduce multipath errors significantly. It also extends the range to the horizon. An altitude of slightly more than 25,000 feet is required to provide a direct line of sight to a horizon 200 n.mi. away. If the relay-aircraft altitude is reduced from 25,000 feet (Fig. 1) to 10,000 feet (Fig. 34), the area enclosed by the multipath error contours doubles. For these reasons the relay-aircraft altitude should be high. A comparison between the contour plots for relay-aircraft

altitudes of 25,000 feet (Fig. 1) and 30,000 feet (Fig. 37) shows only a small improvement in decreasing the area bounded by the contours. Since increasing the relay-aircraft altitude to 30,000 feet and above is quite expensive, and since little is gained in reducing multipath errors, 25,000 feet seems an optimum choice for relay-aircraft altitude.

Table 3
Plots Chosen to Study the Effects of Relay-Aircraft Altitude and Ground-Station Altitude

Figure	System Bandwidth (MHz)	RF *Freq.* (GHz)	Relay-Aircraft Altitude (kft)	Ground-Station Altitude (kft)	Polarization	Sea State	Modulation Technique	Tracking Technique	Ground Station-Antenna Beamwidth (deg)
34	1.00	0.90	10	NA	Horiz.	0	Pulse	Leading edge	NA
35	1.00	0.90	15	NA	Horiz.	0	Pulse	Leading edge	NA
36	1.00	0.90	20	NA	Horiz.	0	Pulse	Leading edge	NA
1	1.00	0.90	25	NA	Horiz.	0	Pulse	Leading edge	NA
37	1.00	0.90	30	NA	Horiz.	0	Pulse	Leading edge	NA
25	1.00	0.90	NA	0.90	Vert.	0	Pulse	Leading edge	6
38	1.00	0.90	NA	1.50	Vert.	0	Pulse	Leading edge	6
39	1.00	0.90	NA	2.10	Vert.	0	Pulse	Leading edge	6
40	1.00	0.90	NA	4.20	Vert.	0	Pulse	Leading edge	6
41	2.00	0.90	NA	0.90	Vert.	0	Pulse	Leading edge	6
42	2.00	0.90	NA	1.50	Vert.	0	Pulse	Leading edge	6
43	2.00	0.90	NA	2.10	Vert.	0	Pulse	Leading edge	6
44	2.00	0.90	NA	4.20	Vert.	0	Pulse	Leading edge	6

The altitude of the ground station has an opposite effect on multipath error. Instead of multipath errors decreasing as the altitude is increased, they increase. This is true over the range of ground-station altitudes available to the EATS. The primary reason for this is the magnitude of the path-length difference. As the ground-station altitude is increased to 4200 feet, the path-length differences increase while reflection coefficients remain high. As can be seen from Figs. 41 through 44, no appreciable reduction in errors can be obtained at 2 MHz bandwidth even for these larger path-length differences. Under these conditions, the error is roughly proportional to the path-length difference. Therefore the errors grow larger. If the altitude could be increased further, eventually the system would begin to resolve the direct and indirect signals and the errors would begin to fall off with increasing altitude as they do for the link from the relay aircraft to the tracked object.

Polarization

Table 4 lists the plots chosen to study the effects of polarization. Vertical polarization is the best choice for both the link from a relay aircraft to the tracked object and the link from the ground station to an aircraft. This is a result of the lower reflection coefficient for vertical polarization in the region of Brewster's angle. For the RF frequency and target geometry considered in this study, the grazing angle is often near Brewster's angle. Since the reflection coefficient is lower in this region, the multipath errors are reduced.

Table 4
Plots Chosen to Study the Effects of
Polarization and Sea State

Figure	System Bandwidth (MHz)	RF Freq. (GHz)	Relay-Aircraft Altitude (kft)	Ground-Station Altitude (kft)	Polarization	Sea State	Modulation Technique	Tracking Technique	Ground Station-Antenna Beamwidth (deg)
1	1.00	0.90	25	NA	Horiz.	0	Pulse	Leading edge	NA
2	1.00	0.90	25	NA	Horiz.	1	Pulse	Leading edge	NA
3	1.00	0.90	25	NA	Horiz.	3	Pulse	Leading edge	NA
4	1.00	0.90	25	NA	Circ.	0	Pulse	Leading edge	NA
5	1.00	0.90	25	NA	Circ.	1	Pulse	Leading edge	NA
6	1.00	0.90	25	NA	Circ.	3	Pulse	Leading edge	NA
7	1.00	0.90	25	NA	Vert.	0	Pulse	Leading edge	NA
8	1.00	0.90	25	NA	Vert.	1	Pulse	Leading edge	NA
9	1.00	0.90	25	NA	Vert.	3	Pulse	Leading edge	NA
10	2.00	0.90	25	NA	Horiz.	0	Pulse	Leading edge	NA
11	2.00	0.90	25	NA	Horiz.	1	Pulse	Leading edge	NA
12	2.00	0.90	25	NA	Horiz.	3	Pulse	Leading edge	NA
13	2.00	0.90	25	NA	Circ.	0	Pulse	Leading edge	NA
14	2.00	0.90	25	NA	Circ.	1	Pulse	Leading edge	NA
15	2.00	0.90	25	NA	Circ.	3	Pulse	Leading edge	NA
16	2.00	0.90	25	NA	Vert.	0	Pulse	Leading edge	NA
17	2.00	0.90	25	NA	Vert.	1	Pulse	Leading edge	NA
18	2.00	0.90	25	NA	Vert.	3	Pulse	Leading edge	NA
45	1.00	0.90	NA	0.90	Horiz.	0	Pulse	Leading edge	6
46	1.00	0.90	NA	0.90	Horiz.	1	Pulse	Leading edge	6
47	1.00	0.90	NA	0.90	Horiz.	3	Pulse	Leading edge	6
25	1.00	0.90	NA	0.90	Vert.	0	Pulse	Leading edge	6
48	1.00	0.90	NA	0.90	Vert.	1	Pulse	Leading edge	6
49	1.00	0.90	NA	0.90	Vert.	3	Pulse	Leading edge	6

On some tracked objects such as missiles the polarization cannot be controlled. The SRI proposal of transmitting and receiving circular polarization on the relay aircraft while receiving and transmitting linear polarization on the tracked object seems to be a good compromise. However range errors will be much larger if the tracked object's antenna is horizontally polarized. These errors can be almost twice that found for the same conditions with vertical polarization. Therefore, when possible, the polarization should be vertical.

Sea State

The plots listed in Table 4 are also those chosen to study the effects of sea state. The effect of various sea states was investigated using a model described by Nathanson [6]. This model exponentially lowers the reflection coefficient as a function of sea state, grazing angle, and RF frequency. As expected, the errors decreased in some regions as the sea state increased.

Modulation Technique

Table 5 lists the plots chosen to study the effects of modulation technique. The results of this study clearly show that modulation techniques with range-resolution capability are better suited for the EATS application. The EATS system operates in a multipath environment which is characterized by large path-length differences at high altitudes. Under these conditions those modulation techniques which can resolve the direct from the indirect signals can give error performance over a major portion of the missile range equal to that in a multipath-free environment. A system such as FM/CW does not, by virtue of its modulating function, resolve the direct and indirect signals. Instead it is an averaging technique. Given enough bandwidth, it will average out the multipath interference. However, even at altitudes where a pulse-modulated system has resolved the direct and indirect signal and is operating near an error-free condition, the FM/CW system must still average out the indirect signal. Under these conditions averaging produces errors which are a small fraction of the path-length difference. Since the path-length difference is large in this region, the error in feet can still be quite large. From a multipath-error consideration, this shortcoming of the FM/CW system makes it less usable in the EATS system. When the path-length differences are small, FM/CW and the pulse-modulated techniques give similar errors when each system uses approximately the same bandwidth.

Table 5
Plots Chosen to Study the Effects of Modulation Technique

Figure	System Bandwidth (MHz)	RF Freq. (GHz)	Relay-Aircraft Altitude (kft)	Ground-Station Altitude (kft)	Polarization	Sea State	Modulation Technique	Tracking Technique	Ground Station-Antenna Beamwidth (deg)
1	1.00	0.90	25	NA	Horiz.	0	Pulse	Leading edge	NA
10	2.00	0.90	25	NA	Horiz.	0	Pulse	Leading edge	NA
19	1.00	0.90	25	NA	Horiz.	0	Pulse	Centroid	NA
22	2.00	0.90	25	NA	Horiz.	0	Pulse	Centroid	NA
23	1.00	0.90	25	NA	Horiz.	0	FM/CW*	NA	NA
24	2.00	0.90	25	NA	Horiz.	0	FM/CW†	NA	NA
25	1.00	0.90	NA	0.90	Vert.	0	Pulse	Leading edge	6
45	2.00	0.90	NA	0.90	Horiz.	0	Pulse	Leading edge	6
50	1.00	0.90	NA	0.90	Vert.	0	Pulse	Centroid	6
51	1.00	0.90	NA	0.90	Vert.	0	FM/CW*	NA	6

*Modulation index = 10; FM = 0.05 GHz.

†Modulation index = 20; FM = 0.05 GHz.

Figure 53 shows a comparison of the multipath performance of the two pulse-modulation tracking techniques and the FM/CW tracking technique. The peak range error is plotted as a function of path-length difference for a fixed bandwidth and relative amplitude. This is similar to the horizontally polarized case. For both pulse-modulation techniques, the errors increase as the path length increases, reach a peak, and then eventually fall off to zero when the pulse resolves the direct and indirect signals. The FM/CW technique has an entirely different error characteristic. As the path-length difference increases, the error similarly increases to a peak but then decays to zero with a damped oscillation.

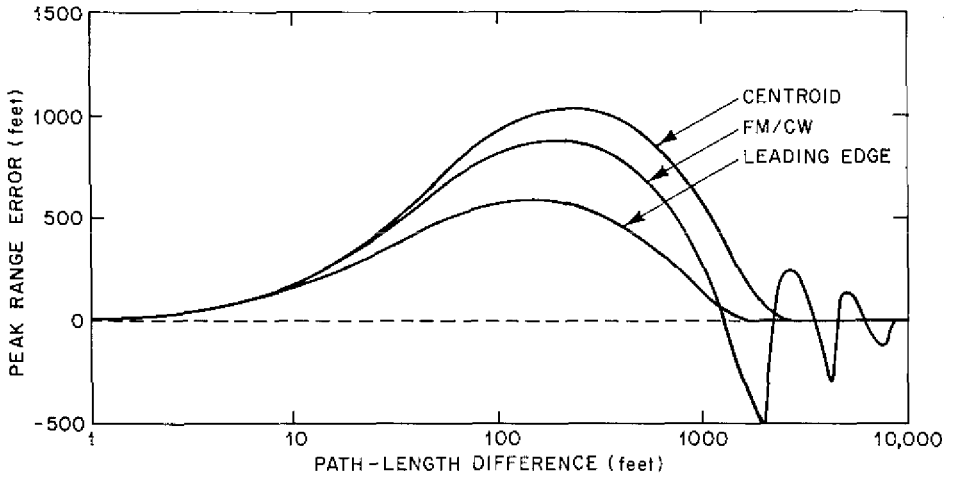

Fig. 53 — Peak errors (bandwidth, 1 MHz; relative amplitude, 0.9; relative phase, 180°)

To explain why errors for the FM/CW system do not diminish like the errors for the pulse-modulation systems, it is convenient to describe the errors on a frequency basis and how the FM/CW system averages as a function of frequency. As described earlier, the range error is a cyclic function of relative phase. The relative phase is equal to the path-length difference expressed in radians at the RF frequency. However the signal transmitted by an FM/CW system consists of a spectrum of frequencies centered about the RF carrier. If a very-narrow-band FM/CW system were used to estimate range, the relative phase would be essentially constant over the transmitted band. This system would yield a range error. If the RF carrier frequency were then changed until one complete cycle of relative phase was observed and the average of all the range errors calculated, the resulting average range error would be zero. This is discussed in more detail in Refs. 3 and 7. If the carrier is changed beyond this point, the average error would again depart from zero. The average will be cyclic, decaying to zero after sufficient change in the RF frequency. The average range error is exactly zero over integer numbers of cycles of relative phase. In an FM/CW system with a fixed bandwidth, an instantaneous average range error is measured over the transmitted frequency spectrum. The transmitted spectrum will average over some whole or fractional number of cycles of relative phase. The number of cycles of relative phase average is related to the system bandwidth and the path-length difference. As the path length increases, more cycles of relative phase are averaged. This process produces the cyclic range errors plotted in Fig. 53.

The processing technique used in ranging with a pulse-modulated system also influences the multipath errors. A leading-edge processor gives significantly better performance against multipath interference than a centroid (center-of-gravity) tracker. This arises because a pulse which is severely distorted by the delayed multipath signal may still have only a slight distortion in the region of its leading edge. Thus its center of gravity may be moved considerably while its leading edge is not moved significantly.

The previous comments on the choice of modulation technique have been based only on reduction of multipath range error. However the choice of modulation cannot be based entirely on multipath considerations. The effects of thermal noise will also increase range errors and will affect each system differently. The cost and complexity of a system will also influence the final choice. This study did not go into detail in these areas; however some comments are needed for completeness. Since the centroid tracker uses all the energy in the transmitted pulse, it will perform best for a given signal-to-noise ratio (S/N). Studies of FM communication systems indicate that at large S/N the FM performance will equal that of the centroid tracker. But, as S/N approaches unity, the FM/CW system degrades rapidly. The leading-edge system uses only the leading edge of the pulse; therefore its performance will be more susceptible to thermal-noise effects. It is expected [2] to require about 3 dB more S/N to equal the accuracy of the centroid tracker, depending on the particular technique used. Thermal-noise considerations would lead to the choice of a centroid tracker as best and an FM/CW system as second choice.

Both the centroid and FM/CW systems will require a phased-locked oscillator or precision timing device onboard all tracked objects. These devices can be expensive and complex. All systems will require an AGC circuit. The leading-edge circuit will require only a good threshold circuit in addition to the AGC circuit. Therefore the leading-edge circuit should prove the simplest and cheapest to implement.

Ground-Station-Antenna Pattern

Table 6 lists the two plots that were compared to show the effect of the ground-station-antenna pattern. Three ground-station-antenna beamwidths were used to determine their effect on multipath range errors. All antenna patterns were simulated with a sin x/x approximation. For a 1-degree beamwidth the errors were less than 10 feet rms at a 200-n.mi. range (hence no plot was generated). As can be seen from Figs. 25 and 52, the amount of coverage area enclosed by the 10-foot contour increases drastically as the beamwidth increases from 6 to 20 degrees. This trend indicates the ground installations should use narrow beamwidths.

Table 6
Plots Chosen to Study the Effects of the
Ground-Station-Antenna Pattern

Figure	System Bandwidth (MHz)	RF Freq. (GHz)	Relay-Aircraft Altitude (kft)	Ground-Station Altitude (kft)	Polarization	Sea State	Modulation Technique	Tracking Technique	Ground Station-Antenna Beamwidth (deg)
25	1.00	0.90	NA	0.90	Vert.	0	Pulse	Leading edge	6
52	1.00	0.90	NA	0.90	Vert.	0	Pulse	Leading edge	20

METHOD FOR CALCULATING RANGE ERROR

Range error at a point in space is calculated in two major steps. First, the strength and time delay of the multipath signal relative to the direct signal are calculated. These quantities, which include an amplitude factor and phase lag associated with the reflection off the earth's surface, define the combined direct and indirect signal which must be tracked. Second, this signal is applied to each range-tracking technique under study to determine the target's apparent range. Then the true range, measured over the direct path, is subtracted from the apparent range to give the range error.

In the first step a 4/3 earth model is used in calculating the amplitude and phase of the reflected signal relative to the direct signal. The multipath geometry is discussed in detail by Reed and Russell [8]. Care has been taken to avoid any approximations used by Reed and Russell which are not valid for the EATS geometry. The amplitude and phase of the indirect signal are calculated from the theoretical complex reflection coefficient which is good only for a smooth sea [8]. The reflection coefficient is calculated for horizontal, vertical, and circular polarization. The theoretical reflection coefficient is modified by a divergence factor to account for reflection from a spherical surface. This factor is discussed in Ref. 8. The antenna pattern of the transmitting antenna also reduces the amplitude of the indirect signal. It is assumed that the antenna axis is pointing along the direct path and that the direct and indirect signals will change in relative amplitude by the amount of difference in antenna gain for their respective direction of propagation. This gain difference is calculated assuming an untapered amplitude distribution over the antenna surface. The expression used to calculate this factor is given by Skolnik [9]. To include the effect of various sea states on the indirect signal, a model described by Nathanson [6] was used. This model applies an exponential weighting to the reflection coefficient which is a function of RF frequency, grazing angle, and height of the ocean waves. The relative phase of the direct and indirect signal is the sum of the phase lag associated with the complex reflection coefficient and the time lag resulting from the longer path of the indirect signal. Once these quantities have been calculated, the signal which is to be processed is known.

In the second step the distorted multipath signal is processed by a computer simulation of the desired tracking system. The calculated range reading of the tracker resulting from this process is then compared to the true range to find the tracking error.

Small movements of the tracked object can produce a large change in relative phase, while the other factors governing the strength of the multipath signal remain essentially constant. For this reason range errors are examined over a 360-degree change in relative phase at each point in space, which will describe a full cycle of the cyclic error. From these data both the rms range error and the peak range error are calculated. The peak error occurs when the relative phase equals 180 degrees.

For calculating rms values the error-versus-phase function is approximated by a discrete set of points. The number of points required to accurately find the rms value for a fixed bandwidth varies with magnitude and time delay of the multipath signal. To minimize computation time, a program was written which examines the amplitude and time-delay values to determine the number of points required for a given accuracy. The resulting error in the estimate of the rms value is less than 10% of its true value.

The rms or peak value of range error can be presented in the form of error contour plots. The multipath error is a reciprocal function; therefore the one-way error has been doubled in the plots to determine the actual two-way error.

METHOD FOR PLOTTING ERROR CONTOURS

Initially a value of the desired rms or peak range error (such as 50 feet) is read by the plotting program. The routine systematically searches at the maximum range of 200 n.mi. for the altitude where this error occurs. This altitude is stored and plotted. The range is then decremented, and a search for the altitude having the desired range error is initiated, starting from the last stored altitude. Once two points have been found and stored in this manner, they are used to predict the starting point for the search at the next range. The prediction is based on the assumption that the contours can be approximated by linear functions over small range intervals. This process is continued until the contour folds back or until a minimum range of 25 n.mi. is reached. If the contour folds back, a special routine increments the altitude and searches for the error in range until the contour has been followed around the tip. After the tip has been traversed, the upper half of the contour is plotted in a manner similar to that described above. This continues until a maximum altitude of 80,000 feet or a maximum range of 200 n.mi. is reached. If the curve does not fold back before 25 n.mi., the lower half is terminated at 25 n.mi. and the upper half is plotted starting at 25 n.mi. and continued to the top or right side of the graph. Each contour curve is labeled with the value of the error (either peak or rms) in feet and an arrow pointing to the upper half of the contour.

This process is repeated for each desired error contour. If the initial search at maximum range does not detect a range error as great as that sought, that contour is assumed missing and all errors are less than that value. This assumption is valid for the link from a relay aircraft to the tracked object. However this assumption is not true for the link from the ground station to a relay aircraft. In the study of the latter link the maximum altitude is only half that used in the study of the link from a relay aircraft to the tracked object. Errors occurring at higher altitudes at the maximum range are missed by this procedure even when these errors extend down into the coverage area at shorter ranges. A more sophisticated starting process would be required to find these contours. However, enough contours are detectable to demonstrate the trends resulting from changing the factors under investigation.

SUMMARY

As predicted by NRL, this study has shown that EATS will have a basic limitation on accuracy because of multipath interference. However the proper system design can minimize the effects of multipath. The original estimate of range error given in Ref. 1 of 9 feet rms must be revised. Under the worst multipath conditions, even with an optimum system, the errors can approach an rms value of 250 feet. These large errors are confined to a small portion of the coverage area, as shown in the contour plots, but do exist and must be considered when predicting the performance of EATS.

The major results of this study are as follows:

- The choice of RF bandwidth has a significant effect on the errors. The errors are approximately halved by using a 2 MHz bandwidth instead of a 1 MHz bandwidth.
- RF frequency has little effect on the magnitude of multipath range errors. However higher RF frequencies do allow the EATS system to reduce multipath errors by time averaging.
- The relay-aircraft altitude chosen should be high to reduce multipath errors. An altitude of 25,000 feet provides good multipath rejection without putting severe requirements on the relay aircraft.
- The EATS polarization should be vertical whenever possible.
- The leading-edge tracking technique is best suited to reduce multipath errors in the EATS application.
- The ground-station-antenna beamwidth should be narrow to reduce multipath. If a 1-degree beam is used, rms errors will be less than 10 feet at a 200-n.mi. range.

ACKNOWLEDGMENT

The author thanks Mr. Jerry Seckel of PMR, who provided valuable background information on the EATS system, and Mr. Chauncey Myers of NRL, who provided analysis programs for FM/CW range errors.

REFERENCES

1. J.F. Cline and J.P. McHenry, "System Requirements for Extended Area Tracking, Target Control and Telemetry at the Pacific Missile Range," Stanford Research Institute, Menlo Park, Calif., Research Memorandum RM-314, July 1973.

2. D.K. Barton and H.R. Ward, *Handbook of Radar Measurement*, Prentice-Hall, Englewood Cliffs, N.J., 1969, Ch. 3.

3. A.M. King, C.M. Morrow, C.G. Myers, and C.L. Moody, "Scintillation Range Noise and Related Phenomena in Water Wave Profiling with Microwave Radar," NRL Report 6641, Sept. 1968.

4. D.D. Howard, "Errors Caused by Complex Sea Surface in a Continuous Height Recording System," NRL Radar Division technical memorandum, May 23, 1956.

5. T.E. Sollenberger, "Multipath Phase Errors in CW-FM Tracking Systems," IRE Trans. on Antennas and Propagation **AP-3** (No. 4), 185-192 (Oct. 1955).

6. F.E. Nathanson, *Radar Design Principles*, McGraw-Hill, New York, 1969, Ch. 1, pp. 33-39.

7. D.C. Cross and J.E. Evans, "Target-Generated Range Errors," NRL Memorandum Report 2719, Jan. 1974.

8. H.R. Reed and C.M. Russell, *Ultra High Frequency Propagation*, 2nd edition, Boston Technical Publishers, Inc., Cambridge, Mass., Chapman and Hall, London, 1966, Ch. 4, pp. 82-115.

9. M.I. Skolnik, editor, *Radar Handbook*, McGraw-Hill, New York, 1970, Ch. 11, p. 10.

Appendix A
RANGE ERROR FOR A PHASE-MODULATED SYSTEM IN A MULTIPATH ENVIRONMENT

A phase-modulated carrier is given by

$$a = A \sin [\omega_c t + (\varphi_0 + \Delta\varphi \cos \omega_\mu t)]. \tag{A1}$$

Without loss of generality, φ_0, the initial phase at $t = 0$, can be assumed equal to 0; then a is given as

$$a = A \sin (\omega_c t + \Delta\varphi \cos \omega_\mu t),$$

where A is the amplitude, ω_c is the carrier in radians per second, $\Delta\varphi$ is the peak phase deviation, ω_μ is the modulating frequency in radians per second, and t is time.

The output of a phase-modulated receiver with a perfect limiter would be the phase deviation function $\Delta\varphi \cos \omega_\mu t$. The modulating function is $\cos \omega_\mu t$. Range information can be obtained by comparing the phase of the transmitted modulation function with the phase of the modulation function detected in the target echo. In the multipath case the phase of the return signal can be distorted and produce a false range indication. The phase-modulation carrier arriving over an indirect path is

$$a_i = b \sin [\omega_c(t - \Delta t) + \Delta\varphi \cos \omega_\mu(t - \Delta t)], \tag{A2}$$

where b is the amplitude of the reflected signal and Δt is the time difference between the direct and the indirect path.

Letting $A = 1$ in Eq. (A1), the direct and indirect signals are given by

$$a = \sin (\omega_c t + \Delta\varphi \cos \omega_\mu t) \tag{A3}$$

and

$$a_i = b \sin [\omega_c(t - \Delta t) + \Delta\varphi \cos \omega_\mu(t - \Delta t)]. \tag{A4}$$

Since a phase-modulated receiver is not sensitive to amplitude change, the important quantity is the instantaneous phase α shown in Fig. A1. As seen in the figure,

$$\alpha = \alpha_1 + \tan^{-1} \left[\frac{b \sin (\alpha_2 - \alpha_1)}{1 + b \cos (\alpha_2 - \alpha_1)} \right] \tag{A5}$$

and

$$\alpha_2 - \alpha_1 = -\omega_c \Delta t + \Delta\varphi \left[\cos \omega_\mu (t - \Delta t) - \cos \omega_\mu t\right]$$

$$= -\omega_c \Delta t + 2\Delta\varphi \sin \omega_\mu \left(t - \frac{\Delta t}{2}\right) \sin \omega_\mu \frac{\Delta t}{2}. \tag{A6}$$

Let

$$\psi_0 = -\omega_c \Delta t,$$

$$B = t - \Delta t/2,$$

$$Z = 2\Delta\varphi \sin \omega_\mu \Delta t/2.$$

Then

$$\alpha_2 - \alpha_1 = \psi_0 + Z \sin B. \tag{A7}$$

The detected phase Φ_D of the received echo including multipath is given by

$$\Phi_d = \tan^{-1} \left[\frac{b \sin (\alpha_2 - \alpha_1)}{1 + b \cos (\alpha_2 - \alpha_1)}\right]$$

$$= -\sum_{n=1}^{\infty} (-1)^n \frac{b^n}{n} \sin [n(\alpha_2 - \alpha_1)]. \tag{A8}$$

Substituting (A7) in (A8) yields

$$\Phi_d = -\sum_{n=1}^{\infty} (-1)^n \frac{b^n}{n} \sin (n\psi_0 + nZ \sin B) \tag{A9}$$

$$= -\sum_{n=1}^{\infty} (-1)^n \frac{b^n}{n} \sin (n\psi_0) \cos (nZ \sin B) + \cos (n\psi_0) \sin (nZ \sin B)$$

$$= -\sum_{n=1}^{\infty} (-1)^n \frac{b^n}{n} \sin (n\psi_0) \left[J_0(nz) + 2 \sum_{n=1}^{\infty} J_{2m}(nz) \cos (2mB)\right]$$

$$-\sum_{n=1}^{\infty} (-1)^n \frac{b^n}{n} \cos (n\psi_0) \left\{2 \sum_{n=0}^{\infty} J_{2m+1}(nz) \sin [(2m + 1) B]\right\}.$$

Removing all components of Eq. (A9) except the term containing the fundamental leaves

$$\Phi_{df} = -\sum_{n=1}^{\infty} (-1)^n \frac{b^n}{n} \cos (n\psi_0) \left[2 J_1(nz) \sin B\right]. \tag{A10}$$

Substituting for ψ_0, B, and z gives

$$\Phi_d = -2\sum_{n=1}^{\infty} (-1)^n \frac{b^n}{n} cos\ (n\omega_c \Delta t) J_1(2\Delta\varphi n\ sin\ \omega_\mu \Delta t/2) sin\ \omega_\mu (t - \frac{\Delta t}{2})$$

$$= -2\sum_{n=1}^{\infty} (-1)^n \frac{b^n}{n} cos\ (n\omega_c \Delta t) J_1(2\Delta\varphi n\ sin\ \omega_\mu \Delta t/2) sin\ \omega_\mu (t - \frac{\Delta t}{2}). \quad (A11)$$

Letting $H_0 = \sum_{n=1}^{\infty} (-1)^n \frac{b^n}{n} cos\ (n\omega_c \Delta t) J_1(2n\Delta\varphi\ sin\ \omega_\mu \frac{\Delta t}{2})$ gives

$$\Phi_d = -2H_0\ sin\ \omega_\mu (t - \frac{\Delta t}{2}). \quad (A12)$$

Therefore, using Eqs. (A5) and (A12),

$$\alpha = \alpha_1 + \Phi_d$$

$$= \Delta\varphi\ cos\ \omega_\mu t - 2H_0\ sin\ \omega_\mu (t - \frac{\Delta t}{2})$$

$$= \Delta\varphi\ cos\ \omega_\mu t - 2H_0\ sin\ \omega_\mu t\ cos\ \omega_\mu \frac{\Delta t}{2} + 2H_0\ cos\ \omega_\mu t\ sin\ \omega_\mu \frac{\Delta t}{2}$$

$$= (\Delta\varphi + 2H_0\ sin\ \omega_\mu \frac{\Delta t}{2})\ cos\ \omega_\mu t - 2H_0\ cos\ \omega_\mu \frac{\Delta t}{2} sin\ \omega_\mu t. \quad (A13)$$

Let

$$\Delta\varphi + 2H_0\ sin\ \omega_\mu \frac{\Delta t}{2} = A\ cos\ \delta$$

and

$$-2H_0\ cos\ \omega_\mu \frac{\Delta t}{2} = A\ sin\ \delta.$$

Then

$$\alpha = cos\ (\omega_\mu t + \delta), \quad (A14)$$

where

$$\delta = tan^{-1}\left[\frac{-2H_0\ cos\ \omega_\mu \frac{\Delta t}{2}}{\Delta\varphi + 2H_0\ sin\ \omega_\mu \frac{\Delta t}{2}}\right] \tag{A15}$$

is the range error in radians, or

$$\delta_t = \frac{1}{\omega_\mu} tan^{-1}\left[\frac{-2H_0\ cos\ (\omega_\mu \frac{\Delta t}{2})}{\Delta\varphi + 2H_0\ sin\ (\omega_\mu \frac{\Delta t}{2})}\right], \tag{A16}$$

where δ_t is range error in seconds.

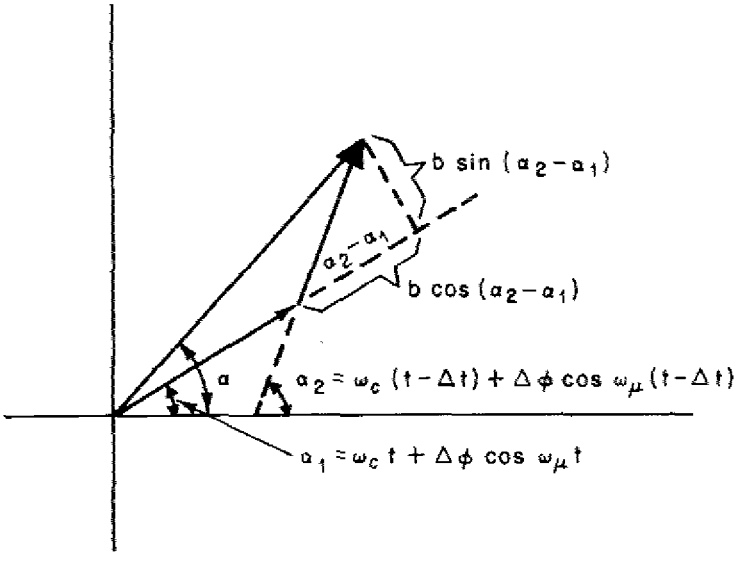

Fig. A1 — Phase relations of the direct and indirect returns